

RNA translational regulation by CPEB4 orchestrates platelet function and pathophysiology

Pilar Navarro

pilar.navarro@iibb.csic.es

Institute of Biomedical Research of Barcelona (IIBB) /CSIC https://orcid.org/0000-0003-4314-4584

Begoña Hurtado

Institute of Biomedical Research of Barcelona (IIBB)/CSIC

Joan Gibert

Hospital del Mar Research Institute (HMRI) https://orcid.org/0000-0002-0742-0759

Núria Vázquez-Bellón

Institute of Biomedical Research of Barcelona (IIBB)/CSIC

Cristina Aresté

Institute of Biomedical Research of Barcelona (IIBB)/CSIC

Agustín Sánchez-Belmonte

Vall d'Hebron Institute of Oncology (VHIO)/Vall d'Hebron https://orcid.org/0000-0001-6936-1873

Pilar Ximénez-Embún

Spanish National Cancer Research Centre (CNIO)

Neus Martínez-Bosch

Hospital del Mar Research Institute (HMRI)

Javier Muñoz

Biocruces Bizkaia Health Research Institute

Dolors Tàssies

Hospital Clínic, Barcelona

Joan Carles Reverter

Hospital Clínic, Barcelona

Albert Morales

Institute of Biomedical Research of Barcelona (IIBB)/CSIC

Raúl Méndez

Institute for Research in Biomedicine (IRB)

Marcos Malumbres

Vall d'Hebron Institute of Oncology https://orcid.org/0000-0002-0829-6315

Pablo García de Frutos

Institute of Biomedical Research of Barcelona (IIBB)/CSIC

Article

Keywords:

Posted Date: January 15th, 2025

DOI: https://doi.org/10.21203/rs.3.rs-5588659/v1

License: © (1) This work is licensed under a Creative Commons Attribution 4.0 International License.

Read Full License

Additional Declarations: There is NO Competing Interest.

RNA translational regulation by CPEB4 orchestrates platelet function and pathophysiology

Begoña Hurtado^{1,2,3#}, Joan Gibert^{4#}, Núria Vázquez-Bellón^{1,5}, Cristina Aresté¹, Agustín Sánchez Belmonte^{2,3}, Pilar Ximénez-Embún⁶, Neus Martínez-Bosch⁴, Javier Muñoz^{6,7,8}, Dolors Tàssies⁹, Joan Carles Reverter⁹, Albert Morales^{1,10,11}, Raúl Méndez^{12,13}, Marcos Malumbres^{2,3,13}, Pablo García de Frutos^{1,10,14*} and Pilar Navarro^{1,4,10*}

- ¹ Department of Cell Death and Proliferation, Institute of Biomedical Research of Barcelona (IIBB)-CSIC, Associated Unit HMRI/IIBB-CSIC, Barcelona, Spain
- ² Cancer Cell Cycle group, Vall d'Hebron Institute of Oncology (VHIO), Vall d'Hebron Barcelona Hospital Campus, Barcelona, Spain
- ³ Molecular Oncology Program, Spanish National Cancer Research Centre (CNIO), Madrid, Spain
- ⁴ Cancer Research Program, Hospital del Mar Research Institute (HMRI), Associated Unit HMRI/IIBB-CSIC, Barcelona, Spain.
- ⁵ PhD Program in Biomedicine, Facultad de Medicina (Campus Clínic), University of Barcelona, Barcelona, Spain
- ⁶ Proteomics Unit, Spanish National Cancer Research Centre (CNIO), 28029 Madrid, Spain.
- ⁷ Cell Signaling and Clinical Proteomics Group, Biobizkaia Health Research Institute,48903 Barakaldo, Spain.
- ⁸ Ikerbasque, Basque foundation for science, 48011 Bilbao, Spain
- ⁹ Haematology Department, Hospital Clínic and University of Barcelona, Barcelona, Spain
- ¹⁰ Institut d'Investigacions Biomèdiques August Pi Sunyer (IDIBAPS), Barcelona, Spain
- ¹¹ Centro de Investigación Biomédica en Red de Enfermedades Hepáticas y Digestivas (CIBEREHD, ISCIII)
- ¹² Institute for Research in Biomedicine (IRB), Barcelona, Spain
- ¹³ ICREA, Barcelona, Spain
- ¹⁴ Centro de Investigación Biomédica en Red de Enfermedades Cardiovasculares (CIBERCV, ISCIII)

[#]These authors contributed equally: Begoña Hurtado, Joan Gibert

^{*}Correspondence to PGF (pablo. garcia@iibb.csic.es) or PN (pilar.navarro@iibb.csic.es)

Abstract

Platelets are highly specialized anucleate cells that play crucial roles in haemostasis, inflammation and disease. Recent data suggest that mRNA translational control is the primary mechanism of gene regulation in platelets. This study unveils a novel pathway to control mRNA translation and protein expression in platelets via the mRNA binding protein CPEB4. We found high CPEB4 expression levels in human and mouse platelets, colocalizing with cytoskeletal proteins. In vivo loss-of-function studies, using the megakaryocytic lineage-specific Pf4-Cre transgenic mice crossed with a strain containing loxP-flanked CPEB4 (Pf4+:Cpeb4-/- mice), revealed a significant reduction of platelet activation and aggregation. These effects were specific to mature platelets, as CPEB4 deficiency did not significantly impact megakaryocytopoiesis. Functional assays, including tail bleeding and collagen-induced embolism, demonstrated impaired coagulation in Pf4+:Cpeb4-/- mice compared to controls. Furthermore, proteomics analysis of resting and activated platelets from Pf4-:Cpeb4+/+ and Pf4+:Cpeb4-/- mice identified distinct molecular signatures of CPEB4-regulated proteins and networks, including those involved in haemostasis and platelet clearance. Our study reveals CPEB4mediated mRNA translational regulation as a novel fine-tuning mechanism for modulating protein synthesis in platelets, with significant functional consequences in both physiological and pathological conditions.

Introduction

Platelets are anucleate cells playing an essential role in haemostasis, thrombosis and inflammation. With a lifespan of 7-10 days, they require continuous renewal from their precursors, megakaryocytes (MKs), to maintain a constant platelet count in the blood. In fact, aberrant platelet counts and/or dysregulated platelet functions are linked not only to cardiovascular diseases but also to conditions such as Alzheimer's disease, autoimmune disorders and cancer^{1–5}.

Under normal conditions, platelets circulate in the bloodstream in a resting, non-adhesive state. However, they can be rapidly activated in response to certain stimuli, in concert with vascular cells and coagulation proteins. This activation involves adhesion, aggregation and secretion processes regulated by complex molecular mechanisms⁶. Traditionally, platelets were thought to lack protein synthesis capability due to their anucleate nature. This belief changed when studies revealed that platelets can stimulate mRNA translation and protein synthesis in response to activation signals. Thus, accumulating evidence demonstrates that platelets can modify their proteome and phenotype through post-transcriptional mechanisms involving mRNA translation. For instance, the mTOR pathway, which promotes cap-dependent mRNA translation, is present in platelets and can be spatially regulated during platelet aggregation^{7–10}. Platelets also regulate 5' UTR mRNA translation initiation after activation through a particular spatial mechanism involving an integrin-mediated redistribution of the capbinding protein eIF4E from the membrane and cytosol to the cytoskeleton^{10,11}.

In addition to 5' UTR-dependent mechanisms, platelet protein expression can be modulated by 3' UTR-dependent translational control. Indeed, platelet transcripts have longer 3' UTRs compared to other cells¹². Moreover, RNA-binding proteins such as TIA-1, TIA-R and HuR, which recognize AU-rich elements in the 3' UTR¹³, and miRNAs are present in platelets^{14–17}, suggesting that 3' UTR-mediated regulation of mRNA translation is crucial for platelet protein expression.

Cytoplasmic polyadenylation element binding proteins (CPEBs) are a family of RNA-binding proteins (CPEB1 to CPEB4) that recognize specific sequences (CPEs, Cytoplasmic Polyadenylation Elements) at the 3' UTR of mRNAs, regulating their polyadenylation, stability and translation^{18,19}. CPEBs were initially identified as key players during early development; in particular, they control the translation of stored maternal mRNAs during oocyte maturation²⁰. Genome-wide studies have revealed that CPEBs may regulate the translation of up to 20% of the vertebrate transcriptome, implicating them in a wide range of biological processes in somatic cells, including cell proliferation, senescence, inflammation and synaptic plasticity^{19,21}. Dysregulation of CPEBs is also associated with pathologies like cancer^{22–28}, neurological disorders^{29–31}, and cardiovascular disease³².

Here, we investigate whether CPEBs regulate mRNA translation and protein expression in platelets to control their biological functions. Our results show that platelets express high levels of CPEB4, which relocates to the cytoskeleton upon thrombin activation. *In vivo*, specific inhibition of CPEB4 in platelets using genetically engineered mice results in reduced platelet activation and aggregation. These effects are associated with impaired

coagulation in CPEB4-deficient mice, leading to increased bleeding in a tail bleeding test and reduced thrombus formation in a collagen-induced embolism assay. Moreover, we use high-throughput mass spectrometry-based proteomics to identify differentially expressed proteins in CPEB4-deficient platelets compared to normal platelets, under both resting and activated conditions. Our study reveals CPEB4-mediated translational control as a novel mechanism to precisely regulate gene expression in platelet biology, both in physiological and pathological conditions.

Results

CPEB4 is expressed in human platelets

The RNA-binding protein family of CPEBs can regulate mRNA translation in several physiological situations where there is no transcription, like cell division^{33,34}, neuronal synapsis³⁵ or terminal erythroid differentiation³⁶. As platelets are anucleate cells where control of RNA stability and/or translation are critical for their functionality, we hypothesized that CPEBs may play a role in this process. To test this hypothesis, we first interrogated public datasets of the human platelet transcriptome³⁷ for CPEBs RNA expression. Interestingly, among the CPEB family, CPEB4 was the most abundant mRNA found in mature human platelets (Fig. 1a). These data were validated by RT-PCR, showing that human platelets contain high CPEB4 mRNA levels in comparison to other CPEB family members (Fig. 1b). CPEB4 expression was confirmed at the protein level by immunoblot analysis from resting and thrombin-activated human platelets' total extracts (Fig. 1c). Moreover, immunoblots from their insoluble fraction showed that CPEB4 was associated with cytoskeleton at very initial stages of thrombin activation, and was partially lost at later stages (Fig. 1d). Interestingly, co-localization of CPEB4 and cytoskeleton was also observed by double immunofluorescence analysis in resting and thrombin-activated human platelets (Fig. 1e).

Together, these *in silico* and *in vitro* findings indicate that, among the four family members of the CPEB genes, CPEB4 is the most abundant in platelets and colocalizes with the cytoskeleton, suggesting a role regulating protein expression and/or biological functions of these cells.

Generation of a platelet-specific mouse model of CPEB4 deficiency

Mouse CPEB family's mRNA expression was studied by interrogating a previously published RNAseq platelet dataset (Rowley et al 2011) (Fig. 2a) and by RT-qPCR analysis (Fig. 2b) from mouse platelets, which confirmed that CPEB4 mRNA was the most abundant member of the family, reproducing the pattern of CPEB expression found in human samples (Fig. 1a,b). CPEB4 protein expression was also confirmed by immunofluorescence in resting and activated mouse platelets (Fig. 2c and Supplementary Fig. S1). In order to explore the specific role of CPEB4 in platelet biology, we used a model of CPEB4 deficiency in mice. For this aim, we generated a mouse strain in which *Cpeb4* gene was deleted in the MK linage. We made use of a previously generated conditional mouse strain, *Cpeb4*^{lox/lox}, ²⁵ and crossed it with Pf4-Cre transgenic animals³⁸, thus generating *Pf4*⁻:*Cpeb4*^{+/+} and *Pf4*⁺:*Cpeb4*^{-/-} mice (Fig. 2d, e). Deficiency

of CPEB4 in platelets from $Pf4^+:Cpeb4^{-/-}$ mice was validated by immunofluorescence (Fig. 2f) and immunoblot (Fig. 2g).

Effects in megakaryocytopoiesis after platelet-specific CPEB4 depletion

GEO2R analysis of human MK transcriptome datasets^{39,40} revealed that CPEB4 is also upregulated during MK differentiation from stem cells (Supplementary Fig. S2a). To evaluate whether CPEB4 deficiency influences platelet formation, we analysed the hemogram and megakaryocytopoiesis of platelets from *Pf4*⁺:*Cpeb4*^{+/+} and *Pf4*⁺:*Cpeb4*^{-/-} mice (Fig. 3; Supplementary Fig. S2). Although total platelet counts were not altered in blood of *Pf4*⁺:*Cpeb4*^{-/-} mice compared to control mice, their plasma levels of thrombopoietin (TPO), the main physiological regulator of MK maturation and platelet production, were significantly higher (Fig. 3a; Supplementary Fig. S2b). We also checked the mean platelet volume (MPV), a value that is inversely correlated to circulating platelet counts (Supplementary Fig. S2c). The MPV/PC ratio was higher in *Pf4*⁺:*Cpeb4*^{-/-} mice than in controls, indicating a reduction in platelet lifespan in the absence of CPEB4 and suggesting that increased TPO levels could mediate a compensatory mechanism to maintain a stable platelet count in the absence of CPEB4 (Supplementary Fig. S2d). No differences were observed in other blood cell counts or parameters (Supplementary Fig. S2e-h).

To explore the possible role of CPEB4 in megakaryocytopoiesis, we analysed bone marrow samples from $Pf4^-:Cpeb4^{+/+}$ and $Pf4^+:Cpeb4^{-/-}$ mice. Staining with anti-von Willebrand Factor (vWF), which is primarily synthesised by MKs, showed an increase in the total number and positive area of MKs per field in $Pf4^+:Cpeb4^{-/-}$ mice (Fig. 3b-c). Nevertheless, analysis of the MK stage by counting mono-, bi- and poly-lobulated cells showed that $Pf4^+:Cpeb4^{-/-}$ MKs presented no differences at any stage (Fig. 3c). The level of phosphorylation of histone H3 at serine 10 (H3S10ph), a marker of mitosis, was similar in both groups (Fig. 3b and 3d), suggesting no general defects in cell division in the bone marrow. Next, we analysed the ploidy of CD41⁺ cells in the bone marrow, in order to check for defects in pro-MK formation (Fig. 3e). No differences were observed between $Pf4^-:Cpeb4^{+/+}$ and $Pf4^+:Cpeb4^{-/-}$ mice, indicating that the increase in the number and size in MKs observed by vWF staining was due to alterations in MK maturation, rather than defects in pro-MK formation.

These data suggest that CPEB4 plays an important role in maintaining platelet homeostasis in blood and that, in its absence, mature MKs and TPO levels increase as a compensatory mechanism.

CPEB4-null platelets show defects in functionality

To study the specific role of CPEB4 in platelet functions, freshly isolated washed platelets from $Pf4^-:Cpeb4^{+/+}$ and $Pf4^+:Cpeb4^{-/-}$ mice were tested for their activation, aggregation and capability of spreading. First, we determined the levels of the platelet α IIb β 3 complex (CD41a) and P-selectin (CD62p), two well characterized factors involved in the binding between platelets and their aggregation. Using flow-cytometry, we observed that CD41a and CD62p were induced in membranes of thrombin-activated platelets from $Pf4^-:Cpeb4^{+/+}$ and $Pf4^+:Cpeb4^{-/-}$ mice (Supplementary Fig. S3a,b). However, the

expression levels of both proteins in these conditions were significantly decreased in *Cpeb4*-null platelets compared to controls, indicating an impairment in platelet activation (Fig. 4a, b). This impairment was also reflected in the kinases AKT and ERK1/2 phosphorylation states, which participate in both platelet inside-out and in the outside-in signalling pathways^{41,42} (Fig. 4c). Soluble washed platelets from $Pf4^-$: $Cpeb4^{+/+}$ and $Pf4^+$: $Cpeb4^{-/-}$ mice were treated with thrombin up to 30 min. Immunoblots showed a significant reduction in the phosphorylation of AKT and ERK1/2, indicating impaired signalling in Cpeb4-null platelets over time. These results could indicate a possible defect in the outside-in signalling pathway (Fig. 4c). Similar results were obtained upon collagen activation of platelets from $Pf4^-$: $Cpeb4^{+/+}$ and $Pf4^+$: $Cpeb4^{-/-}$ mice (Supplementary Fig. S3c).

Next, we interrogated whether this deficit in platelet activation and signalling associates with impaired cell aggregation. Platelets were treated with thrombin for different times and aggregates were determined and quantified by flow cytometry analysis. Depletion of CPEB4 in platelets resulted in a significant decrease of platelet aggregation (Fig. 4d), demonstrating that CPEB4 controls this process.

Finally, we speculated if the observed defects in platelet functionality could also lead to defective platelet spreading, the last step before clot formation on vessel injury. We seeded washed platelets from $Pf4^-:Cpeb4^{+/+}$ and $Pf4^+:Cpeb4^{-/-}$ mice onto a fibrinogen-coated surface, stimulated them with thrombin, allowed them to spread for 30 min and quantified the size of adhered platelets. The area of adhered platelets was decreased in $Pf4^+:Cpeb4^{-/-}$ platelets compared to $Pf4^-:Cpeb4^{+/+}$ platelets (Fig. 4e), indicating that platelets lacking CPEB4 failed to spread as efficiently as wild-type cells.

All together, these results indicate that CPEB4 is involved in platelet biology, controlling platelet activation, aggregation, and signalling pathways in response to pro-coagulant stimuli like thrombin and collagen.

Effects of CPEB4-deficiency in preclinical models of coagulation and thrombosis

To explore the contribution of CPEB4 in haemostasis and its possible implication in thrombosis, we used in vivo preclinical tests modelling coagulation-related pathologies (Fig. 5). First, we used the tail bleeding test, a well-stablished model to determine haemostatic plug formation⁴³. *Pf4*⁺:*Cpeb4*^{-/-} mice displayed increased general bleeding time in comparison to control mice (Fig. 5a), despite both groups spent the same time to stop first bleeding (Fig. 5b). However, *Pf4*⁺:*Cpeb4*^{-/-} mice needed a shorter time to start bleeding again after the first stop (re-bleeding time; Fig. 5c). The two groups had a similar percentage of animals that had re-bleedings (Fig. 5d). According to these results, mice with CPEB4-null platelets showed less stability in the thrombi formed, which could reflect the defects in platelet functionality observed before (Fig. 4).

Furthermore, we evaluated the thrombotic capacity of $Pf4^+:Cpeb4^{-/-}$ mice by inducing pulmonary embolism by intravenous injection of collagen and epinephrine⁴⁴. In this model, 75% of mice lacking CPEB4 in platelets survived for 10 min in contrast to $Pf4^-:Cpeb4^{+/+}$, which died before this point (Fig. 5e, f). This significant protection from pulmonary embolism correlated with a reduced number of thrombi observed in the lungs of $Pf4^+:Cpeb4^{-/-}$ mice (Fig. 5g, h), which were also significantly smaller (Fig. 5i).

These results indicate that CPEB4 not only can play a role in the physiological functions of platelets as regulators of primary haemostasis, but also it is able to modulate platelet activation in a thrombotic disease model.

Proteomic analysis unveils the CPEB4-regulated proteome in platelets.

CPEB4 exerts its functions through the regulation of mRNA translation and stability, ultimately controlling protein levels. To gain further insight into the mechanisms underlying the changes in platelet functionality caused by CPEB4 deficiency, we performed a proteomic analysis on resting and thrombin-activated *Pf4*⁻:*Cpeb4*^{-/-} and *Pf4*⁺:*Cpeb4*^{-/-} platelets (Fig. 6a). This analysis identified 5,713 proteins from a total of 79,943 peptides. For further analysis, we selected the 5,083 proteins that possess transcripts containing a valid 3' UTR sequence. Our proteome data overlap and surpass, in terms of coverage, previous MS analyses of mouse platelet proteomes^{45,46}, underscoring the depth of our analysis (Supplementary Fig. S4a). As expected, normalized expression levels of CPEB4 were markedly reduced in CPEB4-null platelets under both resting and activated conditions (Fig. 6b and Supplementary Fig. S4b).

In resting $Pf4^+:Cpeb4^{-/-}$ platelets, 274 proteins were differentially expressed compared to $Pf4^-:Cpeb4^{+/+}$ platelets, based on an absolute log2 fold change ≥ 0.3 and a $p_{adj} < 0.05$ (Fig. 6c and Suppl. Table S1). Of these, 176 proteins were upregulated and 98 downregulated. To identify potential CPEB4 targets among these differentially expressed proteins, we analysed the 3' UTR of their mRNAs, applying a combinatorial code for CPEB-mediated translational regulation as previously described 47,48. This analysis unveils that CPEB4-mediated regulation of differentially expressed proteins is both direct and indirect, as only one-third of these proteins (91 out of 274, 33.2%) were predicted to be regulated by CPEB4 according to their 3' UTR mRNA sequence (Supplementary Table S2). Among the differentially expressed proteins, 50.5% (46 out of 91) were predicted to be repressed by CPEB4, 24.2% (22 out of 91) activated, and 25.3% (23 out of 91) exhibited a mixed regulatory role.

To investigate the role of CPEB4 in platelet activation, we compared protein expression in thrombin-activated CPEB4-deficient platelets after normalization to resting platelets ($Cpeb4^{-/-}+Thr/Cpeb4^{-/-}$) versus wild-type platelets under the same conditions ($Cpeb4^{+/+}+Thr/Cpeb4^{+/+}$; Fig. 6d). We detected 385 differentially expressed proteins, 254 of which were up-regulated and 131 down-regulated. Of these 385 proteins, 102 (26.5%) were predicted to be CPEB4 targets, displaying repressor (44.1%), activator (25.5%), or mixed (30.4%) roles (Supplementary Table S3), similar to what we observed under resting conditions.

In the resting platelets, GO analyses of these potential CPEB4 targets revealed an enrichment in biological pathways associated to RNA processing, including translation-related processes such as RNA capping or splicing (Fig. 6e; Supplementary Table S4). These findings are consistent with the established role of CPEB4 in RNA regulation. After activation, GO analysis of the predicted CPEB4 targets revealed an enrichment in CPEB4-deficient platelets of pathways associated with fibrinolysis, and negative regulation of haemostasis, coagulation and plasminogen activation (Fig. 6f; Supplementary Table S5).

This suggests that the absence of CPEB4 in platelets after thrombin stimulation may impair platelet clotting capacity, consistent with observed *in vivo* effects.

To validate our proteomic findings, we selected the transmembrane protein CD47 as one of the most differentially expressed proteins between *Pf4*⁻:*Cpeb4*^{+/+} and *Pf4*⁺:*Cpeb4* -/- platelets, both in resting and thrombin-activated conditions. Immunoblot analysis confirmed that CD47 expression was decreased in the insoluble, cytoskeleton-bound fraction of thrombin-activated CPEB4-null platelets compared to platelets expressing CPEB4 (Fig. 6g), in agreement with the proteomic results.

Taken together, the results of the proteomic experiments suggest that CPEB4 deficiency in platelets leads to an impairment of processes important for platelet functionality, which are even more relevant when platelets become activated. These would ultimately lead to an alteration in clot formation and/or resolution, causing an alteration in the thrombotic mechanisms of CPEB4-deficient mice.

To enhance the translational relevance of our findings, we compared our mouse platelet proteomic data with those from Huang et al⁴⁹, which comprises the largest human platelet proteome described to date (5,186 proteins from previously published human platelet proteomics profiles and 1,017 newly identified proteins). We observed a 76,2% overlap between our mouse platelet proteome and this comprehensive human platelet dataset (Fig. 6h). Notably, CPEB4 was identified as one of the proteins common to both human and mouse platelets⁴⁹. Additionally, we analysed published serial analysis of gene expression (SAGE) data from purified human platelets¹². Our analysis revealed that 48% (24 out of 50) of the predicted CPEB4-regulated transcripts in mouse platelets were also found among human platelet transcripts enriched in cytoplasmic polyadenylation element (CPE) motifs identified in the SAGE study¹² (Fig. 6i). Finally, we compared the list of transcripts from our mouse platelets' MS data with recently published human ribosome profiling (RPF) data, which provides a high resolution footprint of active gene translation. Strikingly, 70% of our identified proteins (136 out of 193 candidates) exhibited ribosome occupancy in the human RPF data, further supporting the conservation of CPEB4-mediated translational control between mouse and human platelets (Fig. 6i).

Collectively, these data strongly suggest that CPEB4 plays a conserved role in regulating mRNA translation in both mouse and human platelets.

Discussion

Platelets play crucial roles in haemostasis, thrombosis, and inflammation, relying on precise molecular mechanisms to regulate protein synthesis in response to external stimuli. Historically, platelets were assumed to have minimal or no capacity for protein synthesis due to their lack of a nucleus. However, recent studies have revealed that post-transcriptional regulatory mechanisms in platelets can significantly shape their proteome and influence platelet function⁹. In this study, we uncover a novel layer of post-transcriptional gene expression regulation in platelets orchestrated by the mRNA binding protein CPEB4. Our data demonstrate that CPEB4 is highly expressed in mature platelets, and its specific genetic inhibition in mice leads to a marked reduction in haemostatic capacity and improved thrombosis resolution. These findings highlight

CPEB4 as a central regulator of gene expression through mRNA translation in platelet biology.

Regulating mRNA translation is crucial for gene expression, especially in platelets, which cannot perform transcription. While translation involves several well-regulated stages—initiation, elongation, and termination—, in platelets, research has primarily focused on 5' UTR-dependent mechanisms, leaving the regulation of 3' UTR-dependent mRNA translation understudied^{6,8,14,16}. Our work identifies a previously unknown mechanism of regulation of platelet mRNA translation by the 3' UTR-RNA binding protein CPEB4. Of the four CPEB family members, we found that CPEB4 is predominantly expressed in both mouse and human platelets (Fig. 1,2), indicating its critical role in regulating gene expression to compensate for the absence of transcription in these anucleate cells. Supporting this hypothesis, SAGE analysis revealed an enrichment of CPE elements in human platelet mRNAs, with RT-PCR confirming high CPEB4 expression¹², strengthening the relevance of CPEB-mediated translational in platelet functions.

CPEB4 is best known as a translational activator, promoting polyA tail elongation to enhance mRNA stability and the translation of select mRNAs during cell division^{18-20,50}, cancer^{22,23}, and neurodevelopmental disorders²⁹. However, recent evidence indicates that CPEB4 can also function as a translational repressor in various biological contexts, including erythropoiesis⁵¹, cardiomyocyte function³², and the regulation of immediate early genes in HeLa cells⁵². In our study, proteomic analysis of CPEB4-deficient platelets revealed that CPEB4 regulates a subset of proteins critical for platelet function under both resting and activated conditions. Specifically, 274 and 385 proteins were differentially expressed in resting and activated platelets, respectively. Notably, more proteins were up-regulated than down-regulated in CPEB4-deficient platelets, suggesting a predominant repressor role for CPEB4. Supporting this, predictions using the combinatorial code by *Piqué et al.*⁴⁷ to identify CPEB4-targets (Supplementary Tables S2 and S3) indicate that CPEB4 primarily functions as repressor (50.5% or 44.1% in resting or activated platelets, respectively), though activator or dual roles were also found. These findings suggest that CPEB4's activator/repressor function may adapt to the dynamic demands of protein synthesis during clot formation. In addition to the predicted roles based on the distance between the CPE and the polyA site used in our analysis⁴⁷, CPEB4 activity has been also reported to be dynamically and reversibly modulated by phosphorylation³³. Therefore, future studies are essential to elucidate the molecular events that govern CPEB4's activator or repressor functions in platelets, particularly in response to stimuli such as thrombin.

Among the most interesting proteins differentially expressed following CPEB4 depletion in platelet was CD47. CD47 is a cell surface protein critical for platelet homeostasis, acting as a "don't eat me" signal to prevent clearance by phagocytes⁵³. The CD47 mRNA contains multiple CPE elements, indicating that it is likely a direct target of CPEB4. In CPEB4-deficient platelets, CD47 was downregulated upon thrombin treatment, suggesting that CPEB4 stabilizes CD47 mRNA and/or promotes its translation during platelet activation. This regulation could profoundly impact platelet survival by protecting them from macrophage-mediated phagocytosis. Furthermore, GO Biological Pathways analysis of CPEB4-targets from our proteomic data revealed significant

enrichment of pathways related to impaired coagulation in CPEB4-deficient thrombinactivated platelets, such as negative regulation of plasminogen activation, negative regulation of coagulation and fibrinolysis (Fig. 6f; Supplementary Table S5). These findings align with our previous report that CPEB4 promotes the translational activation of tissue plasminogen activator mRNA in cancer²². Given that platelet-rich clots are typically more resistant to fibrinolysis^{54,55}, CPEB4 regulation of these pathways may explain the decreased clot stability observed in mice with CPEB4-depleted platelets (Fig. 5c) and their heightened resistance to collagen-induced thrombosis (Fig. 5e-i).

An unresolved question in our work is how CPEB4 is regulated during MK development and platelet formation. Ribosome profiling and RNAseq data suggest that the platelet transcriptome is inherited from MK precursors through selective mRNA sorting and regulated mRNA decay⁵⁶. This selective inheritance includes CD47, which is also seen in our analysis. Another mechanism involved in the stability and integrity of platelet mRNAs is the presence of circular RNAs, which are more resistant to degradation than linear RNAs. Circular RNAs are highly enriched in platelets and erythrocytes compared to MKs and other nucleated cells, highlighting their relevance in shaping the transcriptome of anucleate cells⁵⁷. Our *in silico* analysis of previously published data³⁷ shows an upregulation of CPEB4 during megakaryocytopoiesis (Supplementary Fig. S2a), suggesting a pivotal role for this protein in configuring the platelet transcriptome and proteome, likely through its control of mRNA stability. Unlike erythropoiesis, where CPEB4 levels decrease during terminal differentiation⁵¹, CPEB4 remains elevated in mature platelets, pointing to distinct regulatory mechanisms in these two haematological linages.

Local mRNA translation plays a pivotal role in the rapid and spatially regulated production of proteins within specific subcellular compartments, as seen in neurons 20,58 . Similarly, this mechanism allows platelets to rapidly synthesize proteins required for their activation and function, such as those involved in granule secretion, adhesion, and aggregation, to respond quickly to vascular injury and maintain haemostasis. This mechanism is highly linked to the cytoskeleton, which acts as a scaffold for mRNA trafficking and the organization of the translational machinery 59,60 . CPEB proteins have been found to associate with the cytoskeleton $^{61-63}$, influencing mRNA transport and local translation. Our findings demonstrate that CPEB4 associates with the cytoskeleton upon thrombin activation of platelets (Fig. 1c,d), suggesting that it may regulate local mRNA translation in a signal-dependent manner. Interestingly, α IIb β 3 integrin has been shown to mediate outside-in signalling, inducing platelet aggregation and translation of pre-existing mRNAs by targeting eIF4E to mRNA-rich cytoskeletal domains 11 . Future studies should investigate whether this integrin-mediated mechanism also involves the redistribution of CPEB proteins, including CPEB4, following thrombin stimulation.

Precise translational control offers significant advantages to highly specialized cells like platelets, providing a rapid and signal-dependent means of controlling protein expression. This is particularly relevant in pathological conditions such as sepsis⁶⁴. This implies that active regulation of the transcriptome and proteome is taking place under pathological conditions, impacting hemostasis^{65,66}. Our study highlights the essential role of CPEB4 in platelet mRNA translation, unveiling a novel post-transcriptional

regulatory mechanism with important implications in haemostasis and thrombosis. The high expression of CPEB4 in platelets underscores its importance in maintaining platelet function and responding to vascular injury. CPEB4 deficiency leads to profound changes in platelet activation, resulting in decreased clot formation in a collagen-induced pulmonary embolism model (Fig. 5). Our results suggest that CPEB4-mediated mRNA regulation is a crucial mechanism for maintaining a specific set of mRNAs that are relevant during platelet activation. In silico analysis comparing mouse and human platelet proteomes strengthens the translational relevance of our findings, particularly regarding CPEB4's conserved role in platelet biology. The identification of conserved targets across species, including CD47, suggests that CPEB4-mediated regulation may play a similar role in human platelets. However, it is important to recognize that these results are based on computational analyses, and further experimental validation in human samples will be required to confirm these predictions. Given CPEB4's role in platelet activation and clot stability, targeting this protein presents an exciting opportunity for developing therapeutic strategies for bleeding disorders and thrombotic diseases. Future research should focus on delineating the precise mechanisms underlying CPEB4's regulatory functions and its potential as a therapeutic target in platelet-related pathologies.

Methods

Animal model

A conditional platelet loss-of-function model of CPEB4 was generated by crossing the *Cpeb4*^{lox/lox} strain²⁵ with Pf4-Cre transgenic mice³⁸ to generate a megakaryocyte-specific loss of CPEB4 (from now on, Pf4+:*Cpeb4*-/-) and their respective controls (Pf4-:*Cpeb4*+/+). Mice were housed in the pathogen-free animal facility of the Barcelona Biomedical Research Park (PRBB, Barcelona) following the guidelines for ethical conduct in the care and use of animals as stated in the International Guiding Principles for Biomedical Research involving Animals, developed by the Council for International Organizations of Medical Sciences. These animals were observed daily, and sick mice were killed humanely in accordance with the Guidelines for Humane End Points for Animals used in biomedical research. All animal experimentation was approved by the Institutional Ethics Committees of the PRBB (PNM-16-0009/ 16-0009PR1), and the Generalitat de Catalunya (9067).

Murine and human platelet isolation

The isolation of platelets was executed following established procedures as previously delineated⁶⁷. Briefly, mice were subjected to anaesthesia via the intraperitoneal administration of ketamine (at a dosage of 100 mg/kg) and xylazine (at a dosage of 10 mg/kg). Subsequently, whole blood was aseptically collected from the inferior vena cava into a syringe preloaded with acid citrate dextrose (ACD), at a blood to ACD ratio of 9:1 by volume. This mixture was then combined with an equivalent volume of modified HEPES-Tyrode's buffer (140 mM NaCl, 2 mM KCl, 12 mM NaHCO₃, 0.3 mM NaH₂PO₄, 1 mM MgCl₂, 5.5 mM glucose, 5 mM HEPES, 2 mM EGTA, and 0.035% BSA, pH 6.7) and centrifugated at 150 g for 2 min, isolating the platelet-rich plasma (PRP) fraction. To prevent platelet activation, 5 nM of prostaglandin E1 (PGE1; Sigma-Aldrich) was

incorporated into the PRP. Subsequently, platelets were pelleted by centrifugation at 1,500 g for 4 min at 37 °C. The obtained platelet pellets were meticulously resuspended in a modified HEPES-Tyrode's buffer at pH 7.4 without EGTA and BSA, and 0.02 U/mL of apyrase (Grade VII; Sigma-Aldrich) was added. Then, platelets were counted in a haemocytometer and diluted to the specific density of each assay. Unless otherwise indicated, at least 3 mice of 8- to 12-week-old mice were used.

Isolation of human platelets was conducted in accordance with previously established protocols⁶⁷. Briefly, venous blood was aseptically drawn from consenting and healthy human volunteers who had refrained from medication usage for a minimum of 14 days prior to blood collection. The collected blood was anticoagulated using acid citrate dextrose (ACD) at a blood to ACD volumetric ratio of 9:1. After anticoagulation, centrifugation was carried out at 200 g for 20 min, obtaining the PRP fraction. PRP was supplemented with prostaglandin E1 at a concentration of 500 nM, incubated for 10 min at room temperature and centrifuged at 800 g for 20 min. The resultant platelet pellet was washed twice and suspended in a modified HEPES-Tyrode's solution (134 mM NaCl, 2.9 mM KCl, 12 mM NaHCO₃, 0.34 mM NaH₂PO₄, 10 mM HEPES, pH 7.4) enriched with bovine serum albumin (BSA, 3.5 mg/mL) and apyrase (0.02 U/mL), thus facilitating the generation of a standardized and physiologically relevant experimental milieu for subsequent analyses.

RNA expression analysis

Total RNA was isolated using Enza Total RNA Kit (Omega Bio-tek) manufacturer's instructions. RNA was analysed for purity and quantity in a NanoDrop ND-1000 spectrophotometer (NanoDrop Technologies). RNA (1 μ g) was retro-transcribed into cDNA using cDNA Reverse Transcription Kit (Life Technologies). Mouse HPRT and beta actin, and human 18S and beta actin were used as housekeeping genes. qRT-PCR was performed using 20-25 ng of cDNA per sample using platinum SYBR® Green Master mix (Applied Biosystems). All PCRs were performed in duplicate. Relative expression was presented using the $2^{-\Delta\Delta}C_T$ method. Sequences for each pair of primers are listed in Table S6.

Platelet total extracts and cytoskeletal-bound protein fraction

For protein extraction from soluble platelets, two hundred and fifty microliters of platelets at a concentration of 5 x 10^8 platelets/mL were subjected to incubation at 37 °C for varying durations with either 0.05 UI/mL of thrombin, 10 μ M of ADP, or 10 μ g/mL of collagen (Chrono-log). Subsequently, 250 μ L of a 1:1 volume of 2X RIPA lysis buffer (100 mM Tris-HCl pH 8.0; 0.2% SDS, 2% NP-40, 1% sodium deoxycholate) supplemented with a mixture of protease and phosphatase inhibitors (PhosSTOP and Complete Protease Inhibitor Cocktail, Roche Applied Science) were added. For protein extraction of platelets under adhesion conditions, $1x10^9$ platelets/mL were seeded onto 100 μ g/mL of fibrinogen-coated plates. They were allowed to adhere for 5 min at 37°C and the platelets were stimulated for different time points with 0.05 IU/mL of thrombin, 10 μ g/mL of Collagen or 10 μ M of ADP. After that, the non-adhered platelets were aspirated and the activations were stopped by adding 100 μ L of 1X RIPA buffer (50 mM Tris-HCl pH 8.0; 0.1% SDS, 1% NP-40, 0.5% sodium deoxycholate) supplemented with a mixture of protease and phosphatase inhibitors (PhosSTOP and Complete Protease Inhibitor

Cocktail, Roche Applied Science). The platelet homogenate was incubated at 4 °C for 30 min and to facilitate protein extraction and subjected to centrifugation at 13,000 g for a duration of 15 min at 4 °C. The supernatant was carefully collected and the quantification of the total protein content was achieved employing a bicinchoninic acid-based detection method (Pierce).

Fraction analysis of the insoluble protein fraction followed a previously established protocol with certain modifications⁶⁸. To investigate specific fractions of the cytoskeleton, 1×10^9 platelets within a volume of 1 mL were subjected to lysis by the addition of an equal volume of buffer containing 2% Triton X-100 and 100 mM Tris-HCl at pH 7.4 supplemented with a mixture of protease and phosphatase inhibitors (PhosSTOP and Complete Protease Inhibitor Cocktail, Roche Applied Science). Upon lysis, cytoplasmic actin filaments were promptly precipitated through centrifugation at 15,600 g for 4 min, yielding the insoluble Triton X-100 fraction. Subsequently, this insoluble fraction was solubilized using 50 µL of 1X RIPA lysis buffer and then denatured by boiling 98 °C for 10 min with 10 µL of 6X Laemmli Buffer (70% (v/v) 0.5M Tris-HCl-0.4% (w/v) sodium dodecyl sulphate pH 6.8, 30% (v/v) glycerol, 10% (w/v) SDS, 9.3% (w/v) dithiothreitol, 0.012% (w/v) bromophenol blue and 10% (v/v) β -mercaptoethanol). In a parallel approach, assessment of the subcellular distribution of CPEB4 was conducted by probing its presence in the low-speed centrifuge pellet following platelet lysis using 1% Triton X-100. For subsequent analysis, 20 μL of Triton X-100 insoluble fractions were subjected to SDS-PAGE under reducing conditions, following the directions described in the above paragraph.

Immunoblotting

Unless otherwise indicated, 50 μ g of the total protein or 20 μ L of insoluble fraction were subsequently analysed utilizing SDS-PAGE under reducing conditions, and transferred onto a nitrocellulose membrane. Membranes were blocked for 1 h at room temperature with 5% (w/v) of non-fatty milk in TBS-T (50 mM Tris-Cl, 100 mM NaCl, 0.1% Tween-20, pH 7.4) and incubated overnight at 4 °C with the indicated antibodies: anti-mouse CPEB4 (Clone 149C, CNIO, Madrid, Spain); anti-human CPEB4 (Abcam ab224162); anti-Phospho-p44/42 MAPK (ERK1/2) (Thr202/Tyr204) (#9101), anti-p44/42 MAPK (ERK1/2) (#9102), anti-Phospho-AKT (Ser473) [D9E] (#4060), anti-AKT (#9272) from Cell Signalling; anti-human CD47 (20305-1-AP) from Proteintech; anti- α -Tubulin (Clone DM1A, T9026) and anti- β -Actin (clone AC-15, A5441) from Sigma-Aldrich. All membranes were rinsed 3 times with TBS-T and incubated with secondary antibodies conjugated with HPR. Protein detection was done using the ECL Advance Western Blotting Detection System (Amersham Biosciences) and X-ray film exposure, following the recommendations of the manufacturer.

Immunofluorescence analysis

Immunofluorescence using the primary anti-mouse CPEB4 antibody (Clone 149C, CNIO, Madrid, Spain;²³) was first set-up using mouse embryonic fibroblasts (MEFs). MEFs were isolated from E13.5 embryos and analysed using routine cell cycle protocols⁶⁹. For immunofluorescence, cells were seeded at 60 % of confluency onto glass coverslips. At the next day, MEFs were twice with PBS, fixed with 4 % PFA, permeabilized with 0.2% Triton X-100 and blocked in a 10% goat serum (Sigma) solution in PBS for 30 min at room

temperature. Then MEFs were incubated over night at 4 °C with the appropriate primary antibody in a PBS solution containing 10% goat serum. Preparations were washed twice with PBS and incubated with the appropriate secondary antibodies with Alexa Fluor 647 Phalloidin for 1 hour at room temperature. After two washes, preparations were mounted and analysed. Negative control samples included cells stained solely with secondary antibody. The antibody showed specificity in confocal immunofluorescence microscopy, both in mouse embryonic fibroblasts (MEFs; Supplementary Fig. S2), and platelets from control and $Pf4^+$: $Cpeb4^{-/-}$ mice (Fig. 2e).

For immunofluorescence assays involving soluble platelets, samples were prepared at a concentration of 4×108 cells/mL in Tyrode's buffer, pH 7.4, supplemented with 0.02 IU/mL of apyrase. Platelets were activated using 0.05 IU/mL of thrombin at 37 °C in the presence of 2 mM CaCl₂. After activation, resting and activated platelets were fixed with a 1:1 volume of 8% paraformaldehyde for 10 min at 20 °C. Fixed platelets were then subjected to centrifugation at 1,300 g for 4 min, followed by two washes with PBS containing 0.1% BSA. The platelets were allowed to adhere to positive-charged glass slides, and attached cells were permeabilized with 0.5% Triton X-100 in PBS for 3 min. After additional washing steps and blocking with 10% normal goat serum in PBS for 1 hour at room temperature, the platelets were incubated with the appropriate primary anti-mouse CPEB4 (Clone 149C, CNIO, Madrid, Spain) or anti-human CPEB4 (Abcam ab224162). The preparations were washed twice with PBS-T and incubated 1 hour at room temperature with the secondary antibodies together Alexa Fluor 647 Phalloidin. Following further washing and mounting, staining was visualized using a Leica TCS SPE confocal microscope equipped with an HCX APO 100X 1.30 oil U-V-I objective lens and excited with 488 nm and 532 nm solid-state lasers. Parallel control incubations without the primary antibody were conducted.

Platelet spreading

Platelet spreading experiments were conducted in accordance with established protocols⁷⁰. Lab-Tek™ Chamber Slides (Nunc) were coated overnight at 4 °C with 100 μg/mL of human fibrinogen (Sigma-Aldrich) in PBS, pH 8.0. Then, they were washed with PBS and blocked with 5 mg/mL of heat denatured BSA for 2 h at RT, and then washed again. Platelets were suspended at a concentration of 108 platelets/mL in modified Tyrode's buffer supplemented with 1 mM CaCl₂. The platelets were then seeded onto fibrinogen-coated chambers and incubated at 37 °C for 30 min. During these assays, resting cells were incubated 5 min and fixed with 4% PFA and activated platelets were stimulated with 0.05 UI/mL of thrombin (Chromo-log) for 30 min and then fixed with 4% PFA. Chambers were washed twice with PBS, permeabilized with 0.2% Triton X-100 and blocked in a 10% goat serum (Sigma) solution in PBS for 30 min at room temperature. Subsequently, the samples were incubated over night at 4 °C with the appropriate primary antibody in a PBS solution containing 10% goat serum. Preparations were washed twice with PBS and incubated with the appropriate secondary antibodies with Alexa Fluor 647 phalloidin for 1 hour at room temperature. After two washes, preparations were mounted and analysed. Negative control samples included cells stained solely with secondary antibody. Quantitative analysis of cell area was conducted utilizing ImageJ software.

Blood analysis

For whole-blood cell counts, blood sampling was performed from mandibular vein, collecting 100 μ L of blood into EDTA-coated tubes. Then samples were assessed on an automated analyser (Abacus Jr Vet, Vienna, Austria). Plasmatic TPO levels were measured with a Quantikine Mouse Thrombopoietin ELISA Kit (R&D Systems), following the manufacturer's guidelines.

Histological analysis

Sternum bone marrow from eight-weeks old mice, lungs from pulmonary thromboembolism model were fixed in a solution of 4% of paraformaldehyde, embedded in paraffin and cut in 2.5 µm sections. Sections were stained with haematoxylin and eosin (H&E) following standard protocols. For immunohistochemistry, the von Willebrand factor antibody (FVIII, Dako; 1:2000) and the phospho-Histone H3 (Ser10) (Millipore, 06-570; 1:5000) were used. For quantification, sections were examined using an Olympus BX51 microscope equipped with objective lenses (40/0.75, 20/0.4, 10/0.25, and 4/0.1). Sections were examined using a Nikon ECLIPSE 90i microscope using a CFI Plan Apo Lambda 4X/0.2 WB20 and a CFI Plan Apo Lambda 20X/0.75 DIC/N2 WB1.0 and processed using the ImageJ software.

Bone marrow derived megakaryocyte ploidy analysis

For bone marrow derived MK isolation, the tibia and femur were isolated from 8–12-week-old mice and bone marrow was flushed out by the addition of ice-cold PBS buffer (PBS, 0.5% BSA, 5 mM EDTA) through the lumen of the bone. Marrow was mechanically disrupted to achieve single cell suspension followed by filtering through a 40 μ m nylon strainer to remove bone debris and subsequently subjected to erythrocyte lysis. For red blood cell lysis, the bone marrow cell pellet from 1 mouse was resuspended in 1 mL of ACK lysis buffer (150 mM ammonium chloride, 1 mM potassium bicarbonate, 0.1 mM EDTA) and incubated for 1.5 min on ice. The lysis was stopped by the addition of 10 mL PBS buffer and cells were centrifuged at 200 g for 10 min. Cells were counted and subjected directly to surface antigen staining for flow cytometry analysis.

Flow cytometric analysis of DNA content and surface markers of MKs was determined by staining whole bone marrow cells with fluorescein isothiocyanate (FITC)-conjugated anti-CD41 antibody (Clone MWreg30, BD Biosciences,553848) followed by fixation with 1% methanol-free paraformaldehyde at room temperature for 30 min followed by staining with 2 μ g/mL 4′, 6-diamidino-2-phenylindole (DAPI; Sigma-Aldrich) for 1 hour.

Platelet activation and aggregation by flow cytometry assays

To assay the integrin α IIb β 3 (GPIIb/IIIa) activation and P-selectin (CD62P) expression in mice platelets, 100 μ L of 1 x 10⁶ platelets/mL of washed platelets were incubated for 15 min at room temperature with rat anti-mouse-PE-CD41a (JON/A) or rat anti-mouse-FITC-CD62P (Wug.E9) alone (resting) o together 0.05 IU/mL of thrombin (activated). Reactions were stopped by addition of 400 μ l PBS and samples were analysed within 30 min by flow cytometry. The mean fluorescence intensity (MFI) of mutant versus wild-type platelets was used to measure the activated conformation of mouse integrin α IIb β 3 or the levels of P-selectin in the platelet membrane.

For aggregation assays, we follow a previous described protocol with some modifications⁷¹. Mouse whole blood was obtained from inferior cava vein as describe

above and collected in EDTA mouse blood collection tubes. The blood was diluted with 2x volume of HEPES medium (containing 132 mM NaCl, 6 mM KCl, 1 mM MgSO₄, 1.2 mM KH₂PO₄, 20 mM HEPES, pH 7.4, containing 5 mM glucose). Diluted blood was centrifuged 15 min at 50 g, and the collected PRP was diluted in HEPES medium to a final concentration of 50×10^6 platelets/mL. Each sample of PRP was split into 2 and each aliquot was incubated with 1:100 dilution of Anti-Mouse CD9-FITC (Thermo Scientific, MA1-10311) or Anti-Mouse CD9-APC (Abcam, ab82392) monoclonal antibodies for 15 min at room temperature. An additional staining with 1:100 Ter119-PerCP-Cy5.5 (Ly-76) (eBiosciences; 45-5921-82) was performed to stain and gate-out the residual erythrocytes. After incubation, aliquots of PRP were centrifuged 5 min at 2250 g and resuspended in HEPES medium supplemented with 2% (vol/vol) heparin mouse plasma. The 2 populations of labelled washed platelets were mixed 1:1 and then pre-incubated for 5 min at 37 °C while shaking at 600 rpm. Platelets were then activated with 0.05 IU/mL of Thrombin at 37 °C while shaking at 1000. At different times, samples were fixed by addition of 9x volume of 0.5% (vol/vol) formaldehyde (Polysciences Inc., Warrington, NJ, methanol-free) in phosphate-buffered saline. Then, fixed samples were measured by flow cytometry.

In all assays described above, 10,000 platelet-gated events were collected per experiment in a BD FACSCanto™ II cytometer (BD Biosciences). Data were analysed using FlowJo Version 8.8.7 software (TreeStar).

Tail bleeding time

Tail bleeding time measurements were performed as described⁷², with minor modifications. Mice were anesthetized with an i.p. injection of ketamine (100 mg/kg) and xylazine (20 mg/kg). Five mm of the tip of the tail was cut and immediately immersed in PBS pH 7.4 pre-warmed at 37 °C. Bleeding time was defined as the time needed for the stream of blood to cease for 180 s. Monitoring was stopped at 10 min by cauterizing the tip of the tail.

Pulmonary embolism model

To induce thromboembolism, mice were anesthetized with an i.p. Injection of ketamine (100 mg/kg) and xylazine (20 mg/kg) and a mixture of 0.5 mg/kg of collagen (equine collagen; Hormon Chemie) and 60 μ g/kg of epinephrine was injected into the jugular vein of $Pf4^-:Cpeb4^{+/+}$ and $Pf4^+:Cpeb4^{-/-}$ mice and monitored during 15 min. Then, mice were euthanized by cervical dislocation and the lungs collected and processed for histological analysis⁷³.

Sample preparation for proteomic analysis

For proteomic assays, in resting conditions $1x10^8$ platelets/mL from each genotype were pelleted at 1600 g and snap frozen in liquid N_2 . Activated conditions were performed as described in platelet spreading section, with some modifications. In brief, 6-well culture plates were coated overnight at 4 °C with 100 µg/ml Bovine fibronectin (Sigma F4759) in PBS, pH 8.0. Next, the wells were washed with PBS and blocked with 5 mg/ml heat-denatured BSA for 2 hours at RT and then washed again. Platelets at 2 10^8 platelets/ml were incubated on the fibronectin-coated 6-well plate wells in triplicated, and allowed to spread for 45 minutes at 37°C in the presence of 0.1 IU/ml thrombin and 2 nM of CaCl₂. The spreading was also stop snapping frozen the 6-well plates in liquid nitrogen.

Two biological replicates from each condition (resting or thrombin activated) and genotype (Pf4*:Cpeb4*/+ or Pf4*:Cpeb4*/-) were assayed in proteomic experiments. Cells were lysed in 6M urea in 100 mM HCl ph 7.5, supplemented with 1:1000 (v/v) of benzonase (Novagen) and 1:100 (v/v) of HaltTM phosphatase and protease inhibitor cocktail 100x (Thermo Fisher Scientific). Protein concentration was determined using the BCA Protein Assay (ThermoScientific) using BSA as standard. Then, samples (60 μg) were digested by means of the standard FASP protocol. Briefly, proteins were reduced (15 mM TCEP, 30 min, RT) and alkylated (30 mM CAA) for 30 min in the dark and sequentially digested with Lys-C (Wako) (protein:enzyme ratio 1:50, 6 h at RT) and trypsin (Promega) (protein:enzyme ratio 1:100, overnight at 37 °C). Resulting peptides were labeled using iTRAQ® reagent 11-plex following manufacturer's instructions. Samples were mixed in 1:1 ratio based on total peptide amount, which was determined from an aliquot by comparing overall signal intensities on a regular LC-MS/MS run. The final mixture was finally desalted using a Sep-Pak C18 cartridge (Waters).

High pH reverse phase chromatography

The proteome was fractionated by means of high pH reverse phase chromatography using an Ultimate 3000 HPLC system equipped with a sample collector. Briefly, peptides were dissolved in 100 μ L of phase A (10 mM NH4OH) and loaded onto a XBridge BEH130 C18 column (3.5 μ m, 250 mm length and 2.1 mm ID) (Waters). Phase B was 10 mM NH4OH in 90% CH3CN. The following gradient (flow rate of 100 μ L/min) was used: 0-50 min 25% B, 50-54 min 60% B, 54-61 min 70% B. 45 fractions were collected from minute 15, 60 sec/each. 35 single fractions were analyzed along with the pool (1) resulting from the fractions collected at the beginning and at the end of the collecting time.

Mass spectrometry

LC-MS/MS was done by coupling an Ultimate 3000 RSLCnano System (Dionex) to a Q-Exactive HF-X mass spectrometer (ThermoScientific). Peptides were loaded into a trap column (Acclaim PepMapTM 100, 100 μm x 2 cm, ThermoScientific) for 3 min at a flow rate of 10 μl/min in 0.1% FA. Then peptides were transferred to an analytical column (PepMapTM RSLC C18, 2 μm, 75 μm x 50 cm, ThermoScientific) and separated using a 60 min effective linear gradient (buffer A: 0.1% FA; buffer B: 100% ACN, 0.1% FA) at a flow rate of 250 nL/min. The gradient used was: 0-3 min 2% B, 3-5 min 6% B 5-60 min 25% B, 60-63 min 33% B, 63-65 min 45% B, 65-70 min 98% B, 70-80 min 2% B. The peptides were electrosprayed (1.5 kV) into the mass spectrometer through a heated capillary at 320 °C and a Funnel RF level of 40%. The mass spectrometer was operated in a data-dependent mode, with an automatic switch between MS and MS/MS scans using a top 12 method (minimum AGC target 8E3) and a dynamic exclusion of 20 sec. MS (350-1500 m/z) and MS/MS spectra were acquired with a resolution of 60,000 and 45,000 FWHM (200 m/z), respectively. Peptides were isolated using a 1 Th window and fragmented using higher-energy collisional dissociation (HCD) at 35% normalized collision energy. The ion target values were 3E6 for MS (25 ms maximum injection time) and 1E5 for MS/MS (86 ms maximum injection time).

Data analysis of proteomics assays

Raw files were processed with MaxQuant (v 1.6.1.0) using the standard settings against a mouse protein database (UniProtKB/Swiss-Prot, 53,449 sequences downloaded on 2018) supplemented with contaminants. Carbamidomethylation of cysteines was set as a fixed modification whereas oxidation of methionines, protein N-term acetylation and NQ deamidation as variable modifications. Minimal peptide length was set to 7 amino acids and a maximum of two tryptic missed-cleavages were allowed. Results were filtered at 0.01 FDR (peptide and protein level). The "proteinGroup.txt" file was loaded in Prostar package (v1.12.14) (Wieczorek et al. 2017) for further statistical analysis. Reporter intensities were Log2-transformed and normalized using Loess function. Only proteins with a log2 ratio <-0.3 or >0.3 and p-value<0.05 (Limma) were defined as regulated (FDR around 5%). The output was uploaded in Perseus (v1.6.0.7) for further analysis. The proteins differentially expressed were functionally annotated according to Reactome pathways or Biological Processes (both downloaded on 29.01.2019) using ClueGO plugin (v2.5.3) under Cytoscape platform (v3.5.0). Regulated proteins were tested against all the identified proteins (background) using right-sided hypergeometric test. Results were filtered with FDR correction by Bonferroni step down (<5%).

Statistical and bioinformatic analysis

Statistical analyses were performed using Prism software (GraphPad Software). Unless stated otherwise, all statistical tests of comparative data were done using Mann-Whitney test or two-sided, unpaired Student's t tests with Welch's correction when needed, and they are indicated in each Figure. For survival analysis, Log-rank (Mantel-Cox) Test with Bonferroni correction was applied. Data were expressed as means of at least three independent experiments \pm SEM, with P < 0.05 considered statistically significant. Proteomic analysis and visualization were performed with Python (v3.8) using pandas (v2.0.3), numpy (v1.24.3), plotly (v5.9.0) and matplotlib (v3.7.2) packages and R (v4.1.3) using ggrepel (v0.9.1), ggplot2 (v3.3.5) and readxl (v1.4.2) packages. In order to determine potentially direct targets of CPEB4, assessment of the 3' UTR of the identified candidates in the proteomics analysis was performed. First, for each DE protein, the longest 3' UTR corresponding transcript from the reference sequence was selected (Biomart ENSEMBL archive February 2014). To analyse CPE- containing mRNAs, the script developed by Piqué et al.⁴⁷ was used and CPE motifs were counted for each transcript. The full list of CPE detected motifs can be found in Supplementary Tables S2 and S3. A list of CPEB4-targets differentially expressed proteins was submitted to Enrichr for GO Biological Processes enrichment analysis(https://maayanlab.cloud/Enrichr/). The analysis was conducted using the default settings, with pathways ranked by adjusted pvalue to identify significantly enriched terms (Supplementary Tables S4 and S5). Results were visualized using bar plots to highlight the top enriched GO biological processes using the Python packages described above. The cutoff for significance was set at an adjusted p-value of < 0.05, and redundant terms were manually filtered to focus on key pathways relevant to the study.

Data availability

The mass spectrometry proteomics data have been deposited to the ProteomeXchange Consortium via the PRIDE partner repository with the dataset identifier PXD058538. The following username (reviewer_pxd058538@ebi.ac.uk) and password (LNHaYCQSO4gh) can be used during the peer review purposes

References

- 1. Boilard, E. *et al.* Platelets Amplify Inflammation in Arthritis via Collagen-Dependent Microparticle Production. *Science* (1979) **327**, 580–583 (2010).
- 2. Franco, A. T., Corken, A. & Ware, J. Platelets at the interface of thrombosis, inflammation, and cancer. *Blood* **126**, 582–588 (2015).
- 3. Catricala, S., Torti, M. & Ricevuti, G. Alzheimer disease and platelets: how's that relevant. *Immunity & Ageing* **9**, 20 (2012).
- 4. Haemmerle, M., Stone, R. L., Menter, D. G., Afshar-Kharghan, V. & Sood, A. K. The Platelet Lifeline to Cancer: Challenges and Opportunities. *Cancer Cell* **33**, 965–983 (2018).
- 5. Gay, L. J. & Felding-Habermann, B. Contribution of platelets to tumour metastasis. *Nat Rev Cancer* **11**, 123–134 (2011).
- 6. Solari, F. A. *et al.* Multi-omics approaches to study platelet mechanisms. *Curr Opin Chem Biol* **73**, 102253 (2023).
- 7. Weyrich, A. S. *et al.* mTOR-dependent synthesis of Bcl-3 controls the retraction of fibrin clots by activated human platelets. *Blood* **109**, 1975–83 (2007).
- 8. Rowley, J. W., Schwertz, H. & Weyrich, A. S. Platelet mRNA: the meaning behind the message. *Curr Opin Hematol* **19**, 385–391 (2012).
- 9. Zimmerman, G. A. & Weyrich, A. S. Signal-Dependent Protein Synthesis by Activated Platelets. *Arterioscler Thromb Vasc Biol* **28**, (2008).
- 10. Rosenwald, I. *et al.* Expression of Translation Initiation Factors eIF-4E and eIF- 2α and a Potential Physiologic Role of Continuous Protein Synthesis in Human Platelets. *Thromb Haemost* **85**, 142–151 (2001).
- 11. Lindemann, S. *et al.* Integrins Regulate the Intracellular Distribution of Eukaryotic Initiation Factor 4E in Platelets. *Journal of Biological Chemistry* **276**, 33947–33951 (2001).
- 12. Dittrich, M. *et al.* Analysis of SAGE data in human platelets: Features of the transcriptome in an anucleate cell. *Thromb Haemost* **95**, 643–651 (2006).
- 13. Brewer, G. Misregulated posttranscriptional checkpoints: inflammation and tumorigenesis. *J Exp Med* **193**, F1-4 (2001).
- 14. Weyrich, A. S. *et al.* Change in protein phenotype without a nucleus: translational control in platelets. *Semin Thromb Hemost* **30**, 491–8 (2004).
- 15. Dixon, D. A. *et al.* Expression of COX-2 in platelet-monocyte interactions occurs via combinatorial regulation involving adhesion and cytokine signaling. *J Clin Invest* **116**, 2727–38 (2006).
- 16. Neu, C. T., Gutschner, T. & Haemmerle, M. Post-Transcriptional Expression Control in Platelet Biogenesis and Function. *Int J Mol Sci* **21**, (2020).
- 17. Edelstein, L. C. & Bray, P. F. MicroRNAs in platelet production and activation. *Blood* **117**, 5289–96 (2011).

- 18. Ivshina, M., Lasko, P. & Richter, J. D. Cytoplasmic polyadenylation element binding proteins in development, health, and disease. *Annu Rev Cell Dev Biol* **30**, 393–415 (2014).
- 19. Fernández-Miranda, G. & Méndez, R. The CPEB-family of proteins, translational control in senescence and cancer. *Ageing Res Rev* **11**, 460–72 (2012).
- 20. Mendez, R. & Richter, J. D. Translational control by CPEB: a means to the end. *Nat Rev Mol Cell Biol* **2**, 521–9 (2001).
- 21. D'Ambrogio, A., Nagaoka, K. & Richter, J. D. Translational control of cell growth and malignancy by the CPEBs. *Nat Rev Cancer* **13**, 283–90 (2013).
- 22. Ortiz-Zapater, E. *et al.* Key contribution of CPEB4-mediated translational control to cancer progression. *Nat Med* **18**, 83–90 (2011).
- 23. Pérez-Guijarro, E. *et al.* Lineage-specific roles of the cytoplasmic polyadenylation factor CPEB4 in the regulation of melanoma drivers. *Nat Commun* **7**, 13418 (2016).
- 24. Tsai, L.-Y. *et al.* Biphasic and Stage-Associated Expression of CPEB4 in Hepatocellular Carcinoma. *PLoS One* **11**, e0155025 (2016).
- 25. Maillo, C. *et al.* Circadian- and UPR-dependent control of CPEB4 mediates a translational response to counteract hepatic steatosis under ER stress. *Nat Cell Biol* **19**, 94–105 (2017).
- 26. Villanueva, E. *et al.* Translational reprogramming in tumour cells can generate oncoselectivity in viral therapies. *Nat Commun* **8**, 14833 (2017).
- 27. Cao, G., Chen, D., Liu, G., Pan, Y. & Liu, Q. CPEB4 promotes growth and metastasis of gastric cancer cells via ZEB1-mediated epithelial- mesenchymal transition. *Onco Targets Ther* **11**, 6153–6165 (2018).
- 28. Fernández-Alfara, M. *et al.* Antitumor T-cell function requires CPEB4-mediated adaptation to chronic endoplasmic reticulum stress. *EMBO J* **42**, e111494 (2023).
- 29. Parras, A. *et al.* Autism-like phenotype and risk gene mRNA deadenylation by CPEB4 missplicing. *Nature* **560**, 441–446 (2018).
- 30. Parras, A. *et al.* Polyadenylation of mRNA as a novel regulatory mechanism of gene expression in temporal lobe epilepsy. *Brain* **143**, 2139–2153 (2020).
- 31. Picó, S. *et al.* CPEB alteration and aberrant transcriptome-polyadenylation lead to a treatable SLC19A3 deficiency in Huntington's disease. *Sci Transl Med* **13**, eabe7104 (2021).
- 32. Riechert, E. *et al.* Identification of dynamic RNA-binding proteins uncovers a Cpeb4-controlled regulatory cascade during pathological cell growth of cardiomyocytes. *Cell Rep* **35**, 109100 (2021).
- 33. Guillén-Boixet, J., Buzon, V., Salvatella, X. & Méndez, R. CPEB4 is regulated during cell cycle by ERK2/Cdk1-mediated phosphorylation and its assembly into liquid-like droplets. *Elife* **5**, (2016).
- 34. Racki, W. J. & Richter, J. D. CPEB controls oocyte growth and follicle development in the mouse. *Development* **133**, 4527–4537 (2006).

- 35. Si, K. *et al.* A Neuronal Isoform of CPEB Regulates Local Protein Synthesis and Stabilizes Synapse-Specific Long-Term Facilitation in Aplysia. *Cell* **115**, 893–904 (2003).
- 36. Hu, W., Yuan, B. & Lodish, H. F. Cpeb4-Mediated Translational Regulatory Circuitry Controls Terminal Erythroid Differentiation. *Dev Cell* **30**, 660–672 (2014).
- 37. Rowley, J. W. *et al.* Genome-wide RNA-seq analysis of human and mouse platelet transcriptomes. *Blood* **118**, e101–e111 (2011).
- 38. Tiedt, R., Schomber, T., Hao-Shen, H. & Skoda, R. C. Pf4-Cre transgenic mice allow the generation of lineage-restricted gene knockouts for studying megakaryocyte and platelet function in vivo. *Blood* **109**, 1503–1506 (2007).
- 39. Fuhrken, P. G., Chen, C., Miller, W. M. & Papoutsakis, E. T. Comparative, genome-scale transcriptional analysis of CHRF-288-11 and primary human megakaryocytic cell cultures provides novel insights into lineage-specific differentiation. *Exp Hematol* **35**, 476-489.e23 (2007).
- 40. Strassel, C. *et al.* Aryl hydrocarbon receptor–dependent enrichment of a megakaryocytic precursor with a high potential to produce proplatelets. *Blood* **127**, 2231–2240 (2016).
- 41. Patel, P. & Naik, U. P. Platelet MAPKs—a 20+ year history: What do we really know? *Journal of Thrombosis and Haemostasis* **18**, 2087–2102 (2020).
- 42. Guidetti, G. F., Canobbio, I. & Torti, M. PI3K/Akt in platelet integrin signaling and implications in thrombosis. *Adv Biol Regul* **59**, 36–52 (2015).
- 43. Liu, Y., Jennings, N. L., Dart, A. M. & Du, X.-J. Standardizing a simpler, more sensitive and accurate tail bleeding assay in mice. *World J Exp Med* **2**, 30–6 (2012).
- 44. Karpov, A. A., Vaulina, D. D., Smirnov, S. S., Moiseeva, O. M. & Galagudza, M. M. Rodent models of pulmonary embolism and chronic thromboembolic pulmonary hypertension. *Heliyon* **8**, e09014 (2022).
- 45. Zeiler, M., Moser, M. & Mann, M. Copy Number Analysis of the Murine Platelet Proteome Spanning the Complete Abundance Range*. *Molecular & Cellular Proteomics* **13**, 3435–3445 (2014).
- 46. Hurtado, B. *et al.* Thrombocytopenia-associated mutations in Ser/Thr kinase MASTL deregulate actin cytoskeletal dynamics in platelets. *Journal of Clinical Investigation* **128**, 5351–5367 (2018).
- 47. Piqué, M., López, J. M., Foissac, S., Guigó, R. & Méndez, R. A combinatorial code for CPE-mediated translational control. *Cell* **132**, 434–48 (2008).
- 48. Duran-Arqué, B. *et al.* Comparative analyses of vertebrate CPEB proteins define two subfamilies with coordinated yet distinct functions in post-transcriptional gene regulation. *Genome Biol* **23**, 192 (2022).
- 49. Huang, J. *et al.* Assessment of a complete and classified platelet proteome from genome-wide transcripts of human platelets and megakaryocytes covering platelet functions. *Sci Rep* **11**, (2021).
- 50. D'Ambrogio, A., Nagaoka, K. & Richter, J. D. Translational control of cell growth and malignancy by the CPEBs. *Nat Rev Cancer* **13**, 283–90 (2013).

- 51. Hu, W., Yuan, B. & Lodish, H. F. Cpeb4-Mediated Translational Regulatory Circuitry Controls Terminal Erythroid Differentiation. *Dev Cell* **30**, 660–672 (2014).
- 52. Poetz, F. *et al.* Control of immediate early gene expression by CPEB4-repressor complex-mediated mRNA degradation. *Genome Biol* **23**, (2022).
- 53. Olsson, M., Bruhns, P., Frazier, W. A., Ravetch, J. V. & Oldenborg, P.-A. Platelet homeostasis is regulated by platelet expression of CD47 under normal conditions and in passive immune thrombocytopenia. *Blood* **105**, 3577–3582 (2005).
- 54. Weisel, J. W. Structure of fibrin: Impact on clot stability. *Journal of Thrombosis and Haemostasis* vol. 5 Preprint at https://doi.org/10.1111/j.1538-7836.2007.02504.x (2007).
- 55. Napolitano, F. & Montuori, N. Role of Plasminogen Activation System in Platelet Pathophysiology: Emerging Concepts for Translational Applications. *Int J Mol Sci* **23**, 6065 (2022).
- 56. Mills, E. W., Green, R. & Ingolia, N. T. Slowed decay of mRNAs enhances platelet specific translation. *Blood* **129**, e38–e48 (2017).
- 57. Alhasan, A. A. *et al.* Circular RNA enrichment in platelets is a signature of transcriptome degradation. *Blood* **127**, e1–e11 (2016).
- 58. Richter, J. D. Cytoplasmic polyadenylation in development and beyond. *Microbiol Mol Biol Rev* **63**, 446–56 (1999).
- 59. Venticinque, L., Jamieson, K. V & Meruelo, D. Interactions between laminin receptor and the cytoskeleton during translation and cell motility. *PLoS One* **6**, e15895 (2011).
- 60. Piper, M. *et al.* Differential requirement of F-actin and microtubule cytoskeleton in cue-induced local protein synthesis in axonal growth cones. *Neural Dev* **10**, 3 (2015).
- 61. Groisman, I. *et al.* CPEB, maskin, and cyclin B1 mRNA at the mitotic apparatus: implications for local translational control of cell division. *Cell* **103**, 435–47 (2000).
- 62. Huang, Y.-S., Carson, J. H., Barbarese, E. & Richter, J. D. Facilitation of dendritic mRNA transport by CPEB. *Genes Dev* **17**, 638–53 (2003).
- 63. Huang, Y.-S. & Richter, J. D. Regulation of local mRNA translation. *Curr Opin Cell Biol* **16**, 308–13 (2004).
- 64. Middleton, E. A. *et al.* Sepsis alters the transcriptional and translational landscape of human and murine platelets. *Blood* **134**, 911–923 (2019).
- 65. Davizon-Castillo, P., Rowley, J. W. & Rondina, M. T. Megakaryocyte and Platelet Transcriptomics for Discoveries in Human Health and Disease. *Arterioscler Thromb Vasc Biol* **40**, 1432–1440 (2020).
- 66. Huang, J. *et al.* Molecular Proteomics and Signalling of Human Platelets in Health and Disease. *Int J Mol Sci* **22**, (2021).
- 67. Cazenave, J.-P. *et al.* Preparation of washed platelet suspensions from human and rodent blood. *Methods Mol Biol* **272**, 13–28 (2004).

- 68. Jung, S. M. & Moroi, M. Platelet cytoskeletal protein distributions in two triton-insoluble fractions and how they are affected by stimulants and reagents that modify cytoskeletal protein interactions. *Thromb Res* **50**, 775–787 (1988).
- 69. Álvarez-Fernández, M. et al. Greatwall is essential to prevent mitotic collapse after nuclear envelope breakdown in mammals. *Proceedings of the National Academy of Sciences* **110**, 17374–17379 (2013).
- 70. Prévost, N., Kato, H., Bodin, L. & Shattil, S. J. Platelet Integrin Adhesive Functions and Signaling. *Methods Enzymol* **426**, 103–115 (2007).
- 71. De Cuyper, I. M. *et al.* A novel flow cytometry–based platelet aggregation assay. *Blood* **121**, e70–e80 (2013).
- 72. Wonerow, P., Pearce, A. C., Vaux, D. J. & Watson, S. P. A critical role for phospholipase Cgamma2 in alphallbbeta3-mediated platelet spreading. *J Biol Chem* **278**, 37520–9 (2003).
- 73. Angelillo-Scherrer, A. *et al.* Deficiency or inhibition of Gas6 causes platelet dysfunction and protects mice against thrombosis. *Nat Med* **7**, 215–221 (2001).
- 74. Kuleshov, M. V *et al.* Enrichr: a comprehensive gene set enrichment analysis web server 2016 update. *Nucleic Acids Res* **44**, W90-7 (2016).
- 75. Mills, E. W., Wangen, J., Green, R. & Ingolia, N. T. Dynamic Regulation of a Ribosome Rescue Pathway in Erythroid Cells and Platelets. *Cell Rep* **17**, (2016).

Acknowledgements

This work was supported by grants from the Spanish Ministry of Science, Innovation and Universities (MICIU)-Instituto de Salud Carlos III (ISCIII)-European Regional Development Fund (ERDF "A way of making Europe") (PI20/00625 and PI23/00591) to P.N., II Award López-Borrasca 2017 from the Spanish Society for Thrombosis and Hemostasis to P.N. and P.GF., grant from the MICIU-AEI (PID2021-1235640B-100) to P.GF. and A.M., grants from the MICIU-AEI (PID2023-150471NB-I00) and the Spanish Association Against Cancer (AECC) 02547635V to R.M., grant from MICIU-AEI (PDC2022-133408-I00) to M.M., and grant from MICIU-AEI (RED2022-134792-T) to M.M. and R.M. N.V-B. is supported by a FPU ("Formación de Profesorado Universitario") predoctoral contract from the MICIU (FPU21/0928). N. V-B., N.M-B. and P.N. belong to the Spanish National Research Council's Cancer Hub (Conexión Cáncer-CSIC).

Author information

Author contributions

B.H., J.G., D. T., JC. R., A. M., R. M., M. M., P. GF. and P. N. devised the study and designed the experiments. B.H., J.G., N. V-B., C. A., P. X-E., N. M-B., J. M. performed the experiments; J.G. and A. S-B. performed the bioinformatic analysis. B.H., J.G., R. M., M. M., P. GF. and P. N. analyzed the data and wrote the paper. All authors discussed the results, commented on the paper and approved the final version of the manuscript.

B.H. and J.G. contributed equally to this work and shared first authorship. P. GF. and P. N. contributed equally to this work and shared corresponding authorship.

Ethics declarations

Competing interests

The authors declare no conflicts of interest.

Figures

Figure 1

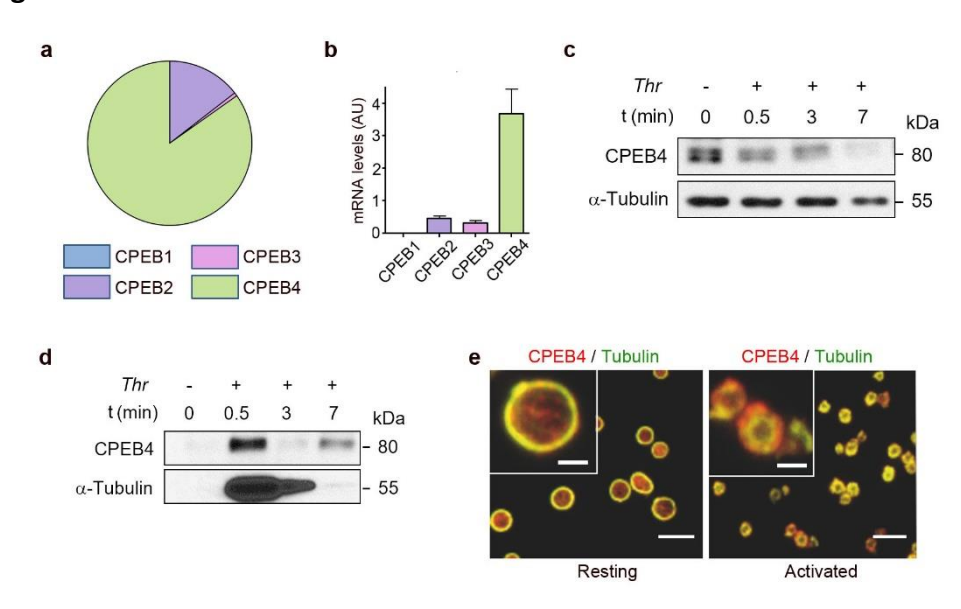


Fig. 1. CPEB4 expression in human platelets. a, Pie charts depicting the transcript per million frequency of the CPEB family members using a human platelet RNAseq dataset³⁷. **b,** Analysis of CPEB1-4 expression by RT-qPCR in human platelets, relative to 18S and ACTB. **c,** Western blot showing CPEB4 protein levels in total extracts from resting human platelets or after activation with thrombin (Thr, 0.05 IU/mL). **d,** Western blot showing CPEB4 protein levels in the insoluble fraction of resting and thrombin-activated human platelets. α-Tubulin is shown as the loading control. **e,** Immunofluorescence showing CPEB4 (red) and tubulin (green) staining in human platelets at resting conditions or after thrombin (0.05 IU/mL) stimulation. Scale bars represent 5 μm (inset, 1 μm).

Figure 2

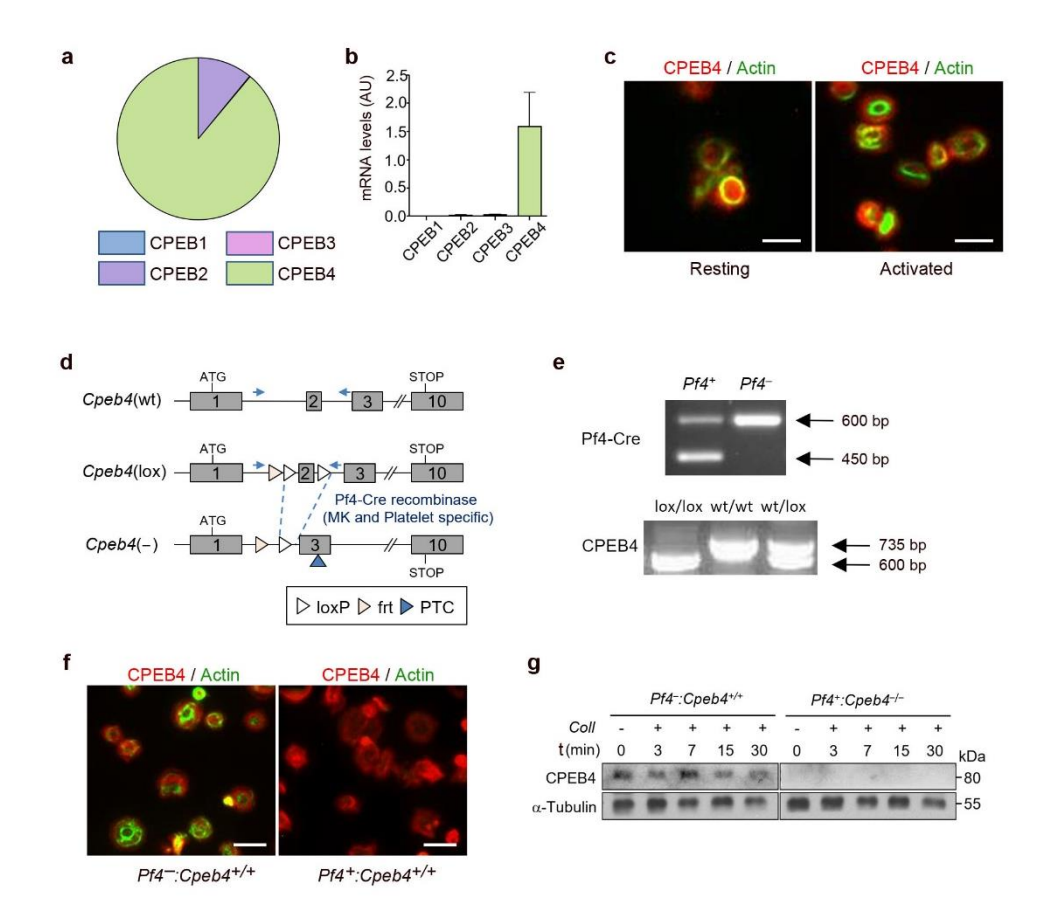


Fig. 2. Generation of a CPEB4-deficient mouse model in platelets. a, Pie charts depicting the transcript per million frequency of the CPEB family members using a mouse platelet RNAseq dataset 8 . b, Analysis of CPEB1-4 expression by RT-qPCR in mouse platelet RNA, relative to 18S and ACTB. c, Immunofluorescence showing CPEB4 (red) and actin (green) staining in mouse platelets at resting conditions or after thrombin stimulation (0.05 IU/mL). Scale bars represent 5 μM. d, Representation of the Cpeb4(wt), Cpeb4(lox) and Cpeb4(–) alleles used in this study. A Pf4-Cre transgene was used to generate MK/platelet-specific Cpeb4-null mice (Pf4+:Cpeb4-/-). The location of the frt, loxP and the new premature termination codon (PTC) are indicated. Blue arrows indicate the primers used for genotyping. e, Visualization on an agarose gel of the PCR products following genotyping of Pf4-Cre (upper panel) and Cpeb4^{lox} (lower panel). f, Immunofluorescence showing CPEB4 (green) and actin (red) staining in Pf4-:Cpeb4+/+ and Pf4+:Cpeb4-/- mouse platelets. Scale bars represent 5 μM. g, Immunoblot showing CPEB4 protein levels in resting or collagen-activated (10μg/mL) mouse platelets from Pf4-:Cpeb4+/+ and Pf4+:Cpeb4-/- mice.

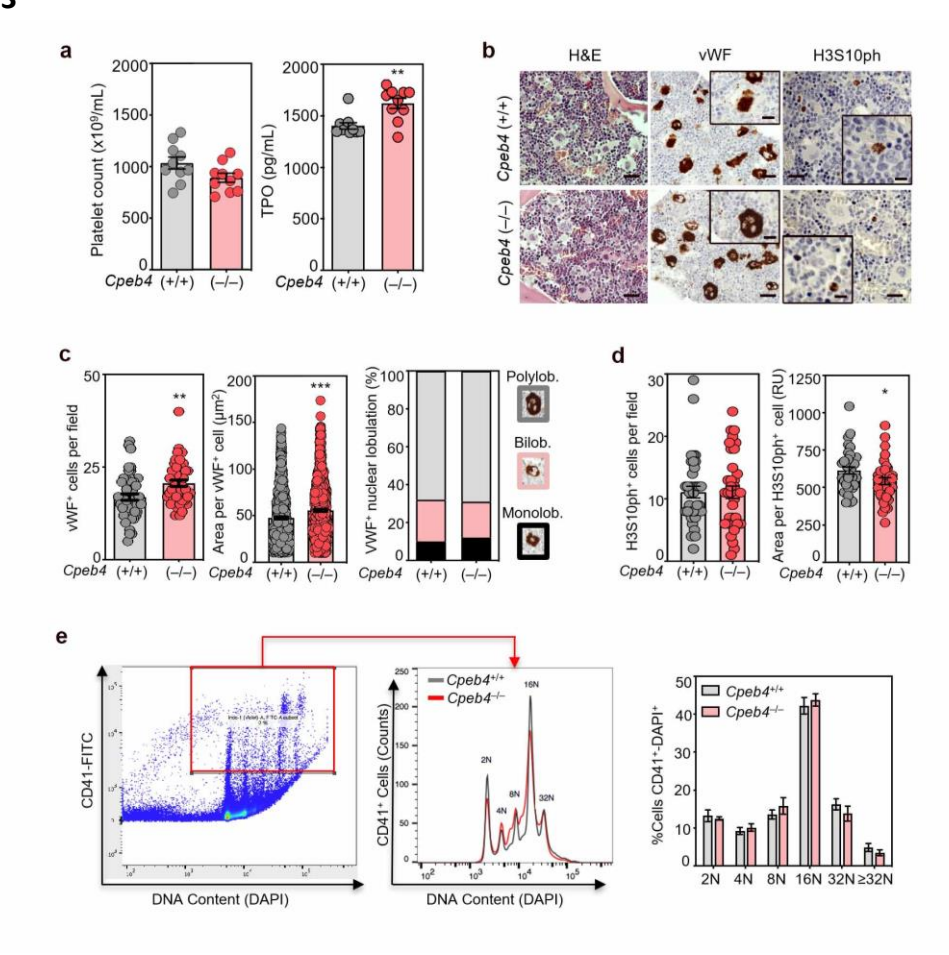


Figure 3. Analysis of megakaryocytopoiesis in Pf4+:Cpeb4-/- mice. a, Platelet and thrombopoietin (TPO) levels in peripheral blood from 8-12-week-old mice with the indicated genotypes (n≥10 mice per genotype). b, Representative haematoxylin and eosin (H&E) staining and immunohistochemistry of von Willebrand factor (vWF) and phosphoS10-histone H3 (H3S10ph) of bone marrow from mice of the indicated genotypes. At least 4 mice per genotype were assessed. Bars represent 10 μm (insets, 5 μm). **c**, Left, bar plots showing number of cells with positive-vWF signal (vWF+) per field and the quantification of the area of vWF positive cells. Right, stacked column plot showing the state of lobulation in the vWF+ cells. At least 12 pictures were analysed from each bone marrow (n=4 mice per genotype). d, Quantification of number of cells (per field) and area of H3S10ph positive cells. At least 10 pictures were analysed from each bone marrow (n=4 mice per genotype). RU, relative units. e, Left, representative flow cytometry plot showing DNA content (DAPI) and CD41+ in Pf4-:Cpeb4+/+ and Pf4+:Cpeb4- $^{\prime-}$ mouse platelets. Right, quantification of the ploidy in CD41+ bone marrow cells from mice of the indicated genotypes (n=5 mice per genotype). Data in all plots show the $mean \pm SEM.*P < 0.05, **P < 0.01, and ***P < 0.001; Unpaired Student's t-test (a, b),$ Mann Whitney test (c, left) and unpaired Student's t test with Welch's correction (c, right and d).

Figure 4

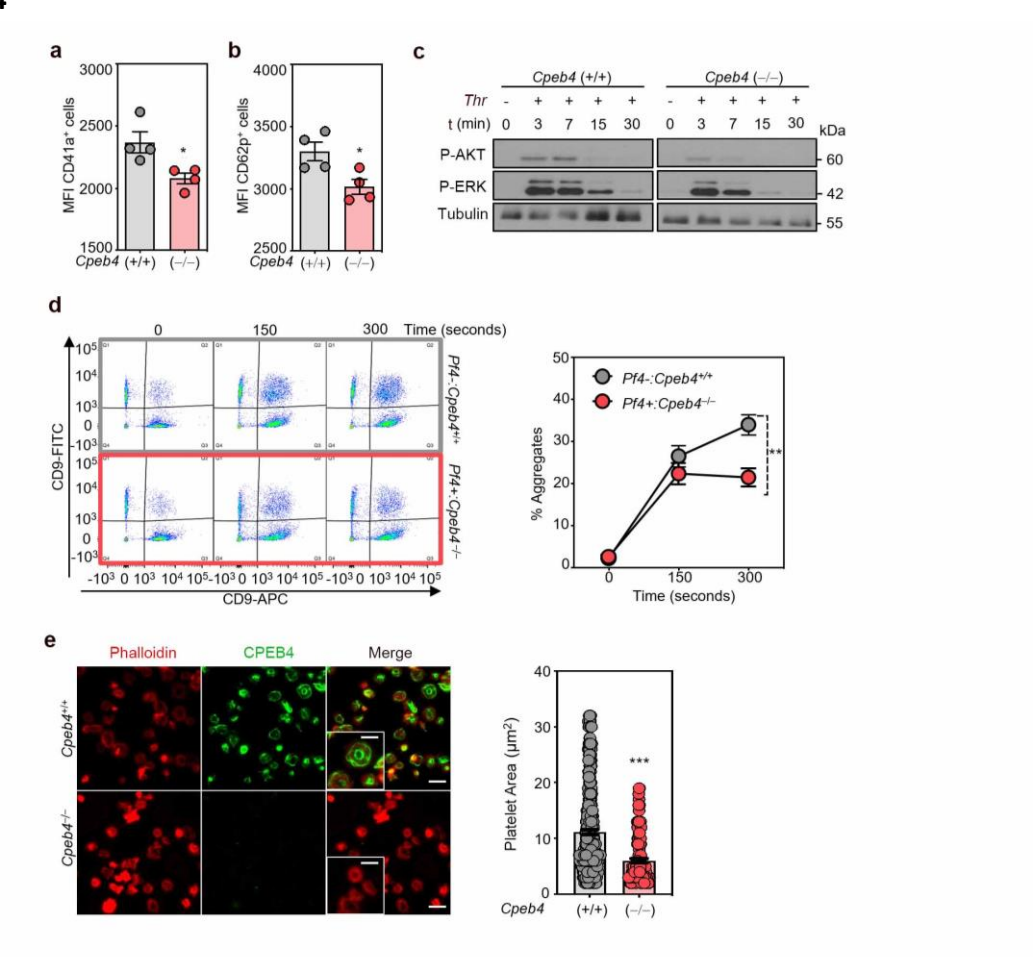


Fig. 4. Analysis of platelet functionality after CPEB4 depletion. a, Analysis of platelet activation by measuring mean fluorescence intensity (MFI) of CD41a+ cells using the conformation-specific antibody JON/A. Bar graph shows MFI in thrombin-activated platelets from Pf4⁻:Cpeb4^{+/+} and Pf4⁺:Cpeb4^{-/-} mice (n=4 mice per genotype). **b**, Analysis of platelet activation by measuring MFI of CD62p+ thrombin-activated platelets from $Pf4^{-}$:Cpeb4^{+/+} and $Pf4^{+}$:Cpeb4^{-/-} mice (n=4 mice per genotype). **c,** Study of AKT and ERK1/2 activation by immunoblot analysis using total protein extracts from soluble platelets in resting (0 min) or thrombin-activated (3-30 min) conditions. Pools of platelets from 3 mice per genotype were used in each condition. **d,** Flow cytometry aggregation assays of washed Pf4⁻:Cpeb4^{+/+} and Pf4⁺:Cpeb4^{-/-} thrombin-activated platelets. Left, representative dot plots from flow cytometry data. Right, quantification of the percentage of aggregates in Pf4-:Cpeb4+/+ and Pf4+:Cpeb4-/- thrombin-activated platelets. **e**, Spreading of Pf4⁻:Cpeb4^{+/+} and Pf4⁺:Cpeb4^{-/-} platelets on fibrinogen. Left, Immunocytofluorescence of platelets stained with Phalloidin (red), for actin labelling, and CPEB4-specific antibody (green). Scale bars: 5 μm (insets: 2.5 μm). Images are representative of 3 independent experiments. Right, bar graph of the quantification of the platelet area according to actin staining. At least, 300 platelets from 4 mice per genotype were analysed. Unless otherwise indicated, data in all plots/graphics shows the mean \pm SEM.*P < 0.05, **P < 0.01, and ***P < 0.001; Unpaired Student's t-test (a,b,d) and Mann-Whitney test (e).

Figure 5

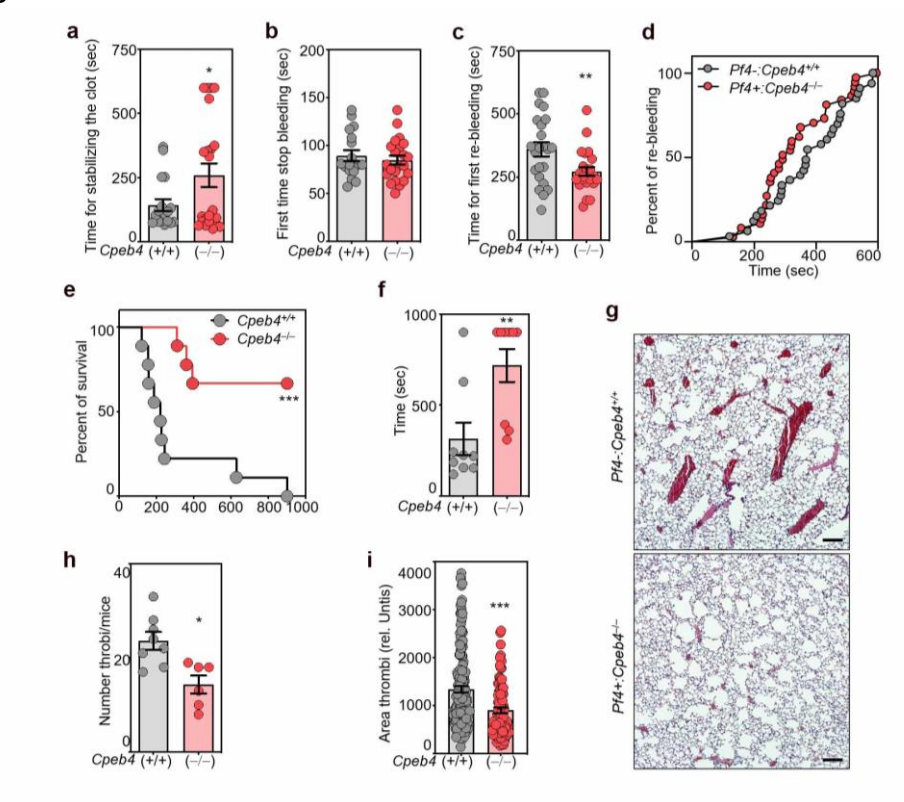


Fig. 5. Effects of CPEB4 depletion in in vivo models of haemostasis and thrombosis. a, Bleeding time for the stabilization of the thrombus of control and $Pf4^+$:Cpeb4 $^{-/-}$ mice, considering stable thrombi those that allow a stoppage of bleeding for more than 180 seconds ($n \ge 18$ per genotype). **b,** Time to stop first bleeding of control and Pf4+:Cpeb4-/mice ($n \ge 18$ per genotype). **c**, Time in which first re-bleeding appears in control and Pf4+:Cpeb4-/- mice (n ≥18 per genotype). **d,** Frequency (%) of mice from each genotype that re-bleed (n ≥18 per genotype). **e,** Survival curve of control and Pf4+:Cpeb4^{-/-} mice after induction of pulmonary embolism using collagen (n = 9 mice per genotype). f, Time in which $Pf4^-$:Cpeb4^{+/+} and $Pf4^+$:Cpeb4^{-/-} mice died after collagen injection (n = 9 mice per genotype). **q,** Hematoxylin and eosin staining of lungs from Pf4⁻:Cpeb4^{+/+} and Pf4+:Cpeb4-/- mice with pulmonary embolism. Scale bars: 50 μ m. **h**, Quantification of number of thrombi in histological images from Pf4⁻:Cpeb4^{+/+} and Pf4⁺:Cpeb4^{-/-} mice (n=8 per genotype). i, Area of thrombi present in histological images from Pf4⁻:Cpeb4^{+/+} and $Pf4^+$:Cpeb4^{-/-} mice (n=8 per genotype). Data in all plots/graphics show the mean \pm SEM. *P < 0.05, **P < 0.01, and ***P < 0.001; Unpaired Student's t-test (a,b,c,f), Log-rank (Mantel Cox) test (d,e), Mann-Whitney test (h), and Student's test with Welch's correction (i), were used.

Figure 6

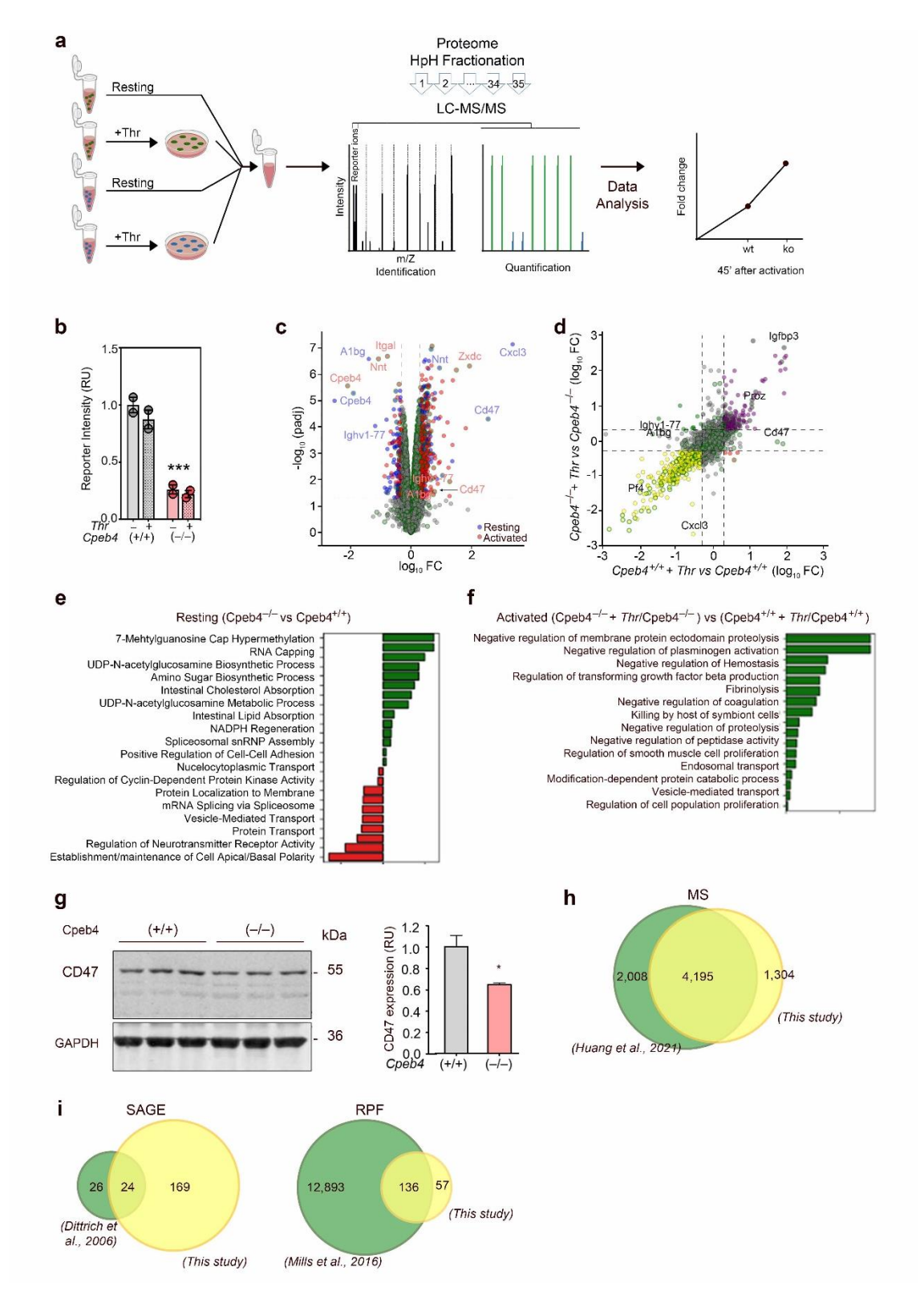


Fig. 6. Proteomic analysis of differentially expressed proteins in platelets from Pf4 $^-$:Cpeb4 $^{+/+}$ and Pf4 $^+$:Cpeb4 $^{-/-}$ mice. a, Schematic representation of the experimental conditions. b, Proteomic validation of CPEB4 detection in resting (–) and thrombinactivated (+) platelets from Pf4 $^+$:Cpeb4 $^{-/-}$ (KO) and Pf4 $^+$:Cpeb4 $^{+/+}$ (WT) mice. CPEB4 is nearly undetectable in KO platelets, serving as a quality control for the proteomics analysis. c, Volcano plot showing differentially expressed proteins in Pf4 $^+$:Cpeb4 $^{-/-}$ versus Pf4 $^-$:Cpeb4 $^{+/+}$ platelets in resting (blue) and activated (red) conditions. d, Scatter plot of

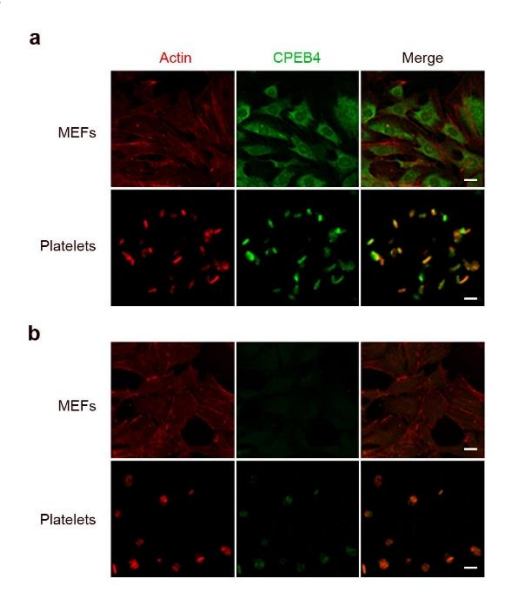
differential protein expression from Pf4+:Cpeb4-/- versus Pf4-:Cpeb4+/+ thrombinactivated platelets with respect to their resting state. **e**, GO Biological Processes enrichment analysis of CPEB4-regulated proteins differentially expressed in Pf4+:Cpeb4-/- versus $Pf4^-$:Cpeb4+/+ resting platelets. Analysis was performed with Enrichr⁷⁴, using as cut off values an adjusted p-value of <0.05. f, GO Biological Processes enrichment analysis of CPEB4-regulated proteins differentially expressed in Pf4+:Cpeb4-/- versus Pf4-: $Cpeb4^{+/+}$ thrombin-activated platelets, normalizing to the resting state proteome. Analysis was performed as in e. g, Immunoblot analysis of platelet extracts showing that CD47 expression was reduced in the insoluble fraction of $Pf4^+$: Cpeb4 $^{-/-}$ platelets. GAPDH is shown as the loading control. Quantification is shown on the right. h, Venn diagrams comparing our mouse platelet proteomic results with previous studies on the human platelet proteome⁴⁹. **i,** Venn diagrams showing the overlap of the CPEB4-targets identified in the present proteomic analysis with human platelet transcripts enriched in CPE motifs identified by SAGE analysis by Dittrich et al. 12 (left) or with human platelet actively translated RNAs identified by ribosome profiling by Mills et al. 75 (right). FC, fold change; GO, gene ontology; Thr, thrombin; MS, mass spectrometry; SAGE, serial analysis of gene expression; RPF, ribosome profiling.

Additional information

Supplementary information Supplementary Figs. S1- S5 Supplementary Tables S1 -S6

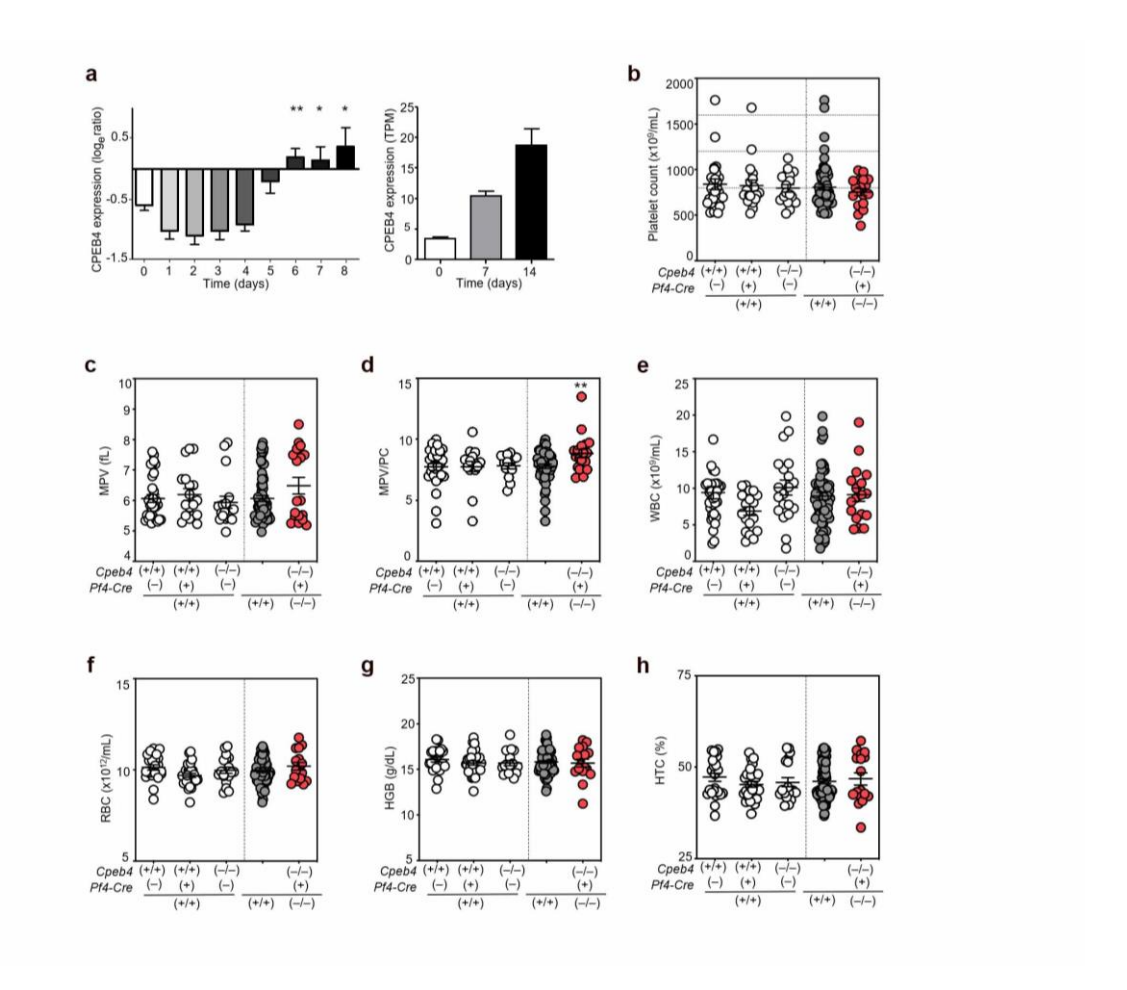
Supplementary Figures

Supplementary Fig. S1



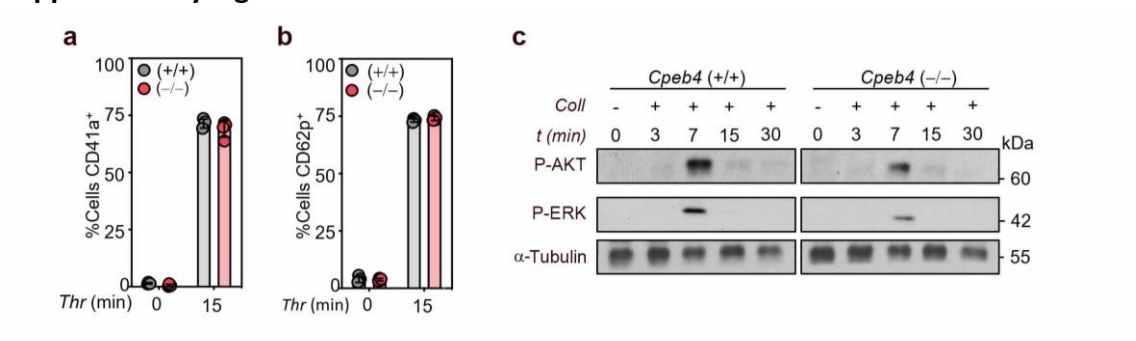
Supplementary Fig. S1. Generation and specificity of the anti-mouse CPEB4 antibody. **a,** Immunofluorescence images showing CPEB4 (green) and actin (red) staining by means of the 149C monoclonal antibody (1:50) in a cell culture of mouse embryonic fibroblasts (MEFs) (upper panels) and mouse platelets (bottom). MEFs showed a cytoplasmatic pattern, whereas in mouse platelets CPEB4 appeared to be localized in cytoskeletal structures. **b,** Negative control images in the absence of primary antibody showing actin staining with Alexa Fluor 647-phalloidine. Note that some platelets display unspecific staining. Scale bars, 5µm.

Supplementary Fig. S2



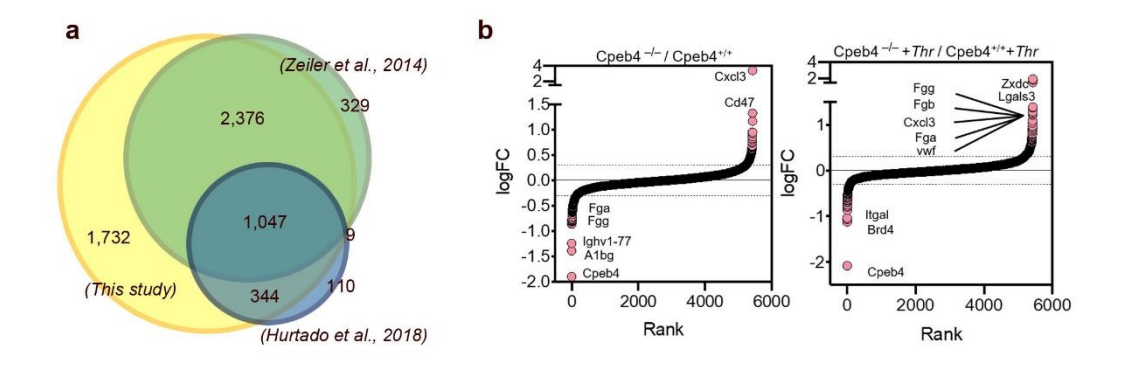
Supplementary Fig. S2. a, CPEB4 expression using RNAseq datasets showing sequential differentiation of CD34+ human stem cells to megakaryocytes (left, GSE3839; right, GSE167866). (**b-h**) Cellular parameters in peripheral blood from 8-12-week-old mice in the different genotypes used to generate Pf4+:Cpeb4-/-mice. **b,** Platelet counts. **c,** Mean platelet volume (MPV). **d,** Ratio between MPC and platelet count (PC) in each mouse. **e,** White blood cells counts (WBC). **f,** Red blood cells counts (RBC). **g,** Levels of hemoglobin. **h,** Percentage of hematocrit (HTC). Unless otherwise indicated, data in all plots/graphics shows the mean \pm SEM. n≥10 mice per genotype. **P < 0.01, Unpaired Student's t-test was used for the comparisons.

Supplementary Fig. S3



Supplementary Fig. S3. a, Percentage of CD41a positive cells, measured by flow cytometry, in resting (0 min) and thrombin activated conditions (15 min); **b,** Percentage of CD62p positive cells, measured by flow cytometry, in resting (0 min) and thrombin activated conditions (15 min); **c,** Analysis of AKT and ERK pathways activation by immunoblot after collagen activation of platelets from Pf4⁻:Cpeb4^{+/+} and Pf4⁺:Cpeb4^{-/-} mice.

Supplementary Fig. S4



Supplementary Fig. S4. a, Venn plot diagram showing overlapping between our results (n=5,499) and previous MS analysis of mouse platelet proteomes: Hurtado et al. 2018 (n=1,510); Zeiler et al 2014 (n=3,761) b, Rank plot of differentially expressed proteins in the MS proteomic analysis of platelets from Pf4+:Cpeb4-/- and Pf4-:Cpeb4+/+ mice under resting (left) and thrombin-activated (right) conditions. Notably, CPEB4 was significantly downregulated in Pf4+:Cpeb4-/-platelets in both conditions, serving as an expected quality control.

Supplementary Tables

Supplementary Table S1. Proteomic analysis of mouse platelets from $Pf4^+:Cpeb4^{-/-}$ and $Pf4^-:Cpeb4^{+/+}$ mice. (excel file)

Supplementary Table S2. Genes predicted as CPEB4 targets from the proteome dataset of mouse resting platelets. (excel file)

Supplementary Table S3. Genes predicted as CPEB4 targets from the proteome dataset of mouse activated platelets. (excel file)

Supplementary Table S4. GO Biological Processes enrichment analysis of CPEB4 targets differentially expressed in $Pf4^+$: Cpeb4 $^{-/-}$ versus $Pf4^-$: Cpeb4 $^{+/+}$ resting platelets (excel file).

Supplementary Table S5. GO Biological Processes enrichment analysis of CPEB4 targets differentially expressed in $Pf4^+:Cpeb4^{-/-}$ versus $Pf4^-:Cpeb4^{+/+}$ thrombin-activated platelets, normalizing to the resting state proteome (excel file).

Supplementary Table S6. Primer sequences used for RT-qPCR.

| Gene | Forward primer (5'- 3') | Reverse primer (5'- 3') |
|-------------|-------------------------|--------------------------|
| Mouse HPRT | CTGGTGAAAAGGACCTCTCGAAG | CCAGTTTCACTAATGACACAAACG |
| Mouse ACTB | CATTGCTGACAGGATGCAGAAGG | TGGAGGTGGACAGTGAGG |
| Human 18S | CCGAAGATATGCTCATGTGG | GTGCGGCTGCTTCCATAAG |
| Human ACTB | AGAAAATCTGGCACCACACC | AGAGGCGTACAGGGATAGCA |
| Mouse CPEB1 | TTCCCAGCACCCTCAGTTAG | ACCCAACGCCCATCTTTAGA |
| Mouse CPEB2 | GGGGCTCAGATTCACTCCAA | TCGTGCTCTGCTCATGAT |
| Mouse CPEB3 | GAGATCACTGCCAGCTTTCG | GGCAGGCATCTATCAGAGCT |
| Mouse CPEB4 | AGGGCTGAACGGTGGAATAA | TGAGTGCATGTCAAACGTCC |
| Human CPEB1 | TCGATCTAGCAGCCCCTCT | CAGCTTGCTCTTGGTCCATC |
| Human CPEB2 | CAAAATGGAGAGCGAATAGAACG | CCAATCTACTACCAAAGGCCC |
| Human CPEB3 | AGGTGTTTGTTGGAGGACTTC | TTTCAGCTTTGTGAGGCCAG |
| Human CPEB4 | TCTGTGCAGGCTCTCATTGA | TGGGTCAAGTGGCTGTGAA |

Supplementary Files

This is a list of supplementary files associated with this preprint. Click to download.

- SupplementaryTableS1Proteomics.xlsx
- SupplementaryTableS2DErestingmouseplateletsCPEprediction.xlsx
- SupplementaryTableS3DEactivatedmouseplateletsCPEprediction.xlsx
- SupplementaryTableS4GOCPEBtargetsDEKOvsWTresting.xlsx
- SupplementaryTableS5GOCPEBtargetsDEKOvsWTactivated.xlsx